A Gigantic, Exceptionally Complete Titanosaurian Sauropod Dinosaur from Southern Patagonia, Argentina

Kenneth J. Lacovara, Matthew C. Lamanna, Lucio M. Ibiricu, Jason C. Poole, Elena R. Schroeter, Paul V. Ullmann, Kristyn K. Voegele, Zachary M. Boles, Aja M. Carter, Emma K. Fowler, Victoria M. Egerton, Alison E. Moyer, Christopher L. Coughenour, Jason P. Schein, Jerald D. Harris, Rubén D. Martínez, Fernando E. Novas

Supplementary Information:

1. Institutional abbreviations

AODF, Australian Age of Dinosaurs Museum, Winton, Australia; **CGM**, Egyptian Geological Museum, Cairo, Egypt; **FMNH**, Field Museum of Natural History, Chicago, U.S.A.; **HIII**, Henan Geological Museum, Zhengzhou, China; **HMN**, Museum für Naturkunde der Humboldt Universität, Berlin, Germany; **MCF-PVPH**, Museo Carmen Funes, Plaza Huincul, Argentina; **MLP**, Museo de La Plata, La Plata, Argentina; **MPM**, Museo Padre Molina, Río Gallegos, Argentina; **MUCPv**, Museo de la Universidad Nacional del Comahue, Neuquén, Argentina; **MZSP**, Museu de Zoologia da Universidade de São Paulo, São Paulo, Brazil; **PVL**, Fundación-Instituto Miguel Lillo, Tucumán, Argentina; **TMM**, Texas Memorial Museum, Austin, U.S.A.; **UNPSJB**, Universidad Nacional de la Patagonia San Juan Bosco, Comodoro Rivadavia, Argentina; **USNM**, National Museum of Natural History, Washington, D.C., U.S.A.; **ZPAL**, Institute of Paleobiology, Polish Academy of Sciences, Warsaw, Poland.

2. Geologic context of *Dreadnoughtus*

The Cerro Fortaleza Formation[2] is located in Santa Cruz Province in southern Argentina, where it is exposed along the Río La Leona between Lago Argentino and Lago Viedma[3-5] (Supplementary Fig. 1). Because the *Dreadnoughtus schrani* quarry is located within the type section of the Cerro Fortaleza Formation, its lithostratigraphic assignment is clear. Stratigraphic

nomenclature has, however, been applied inconsistently across the region (cf. Egerton[6]), and in some studies Cerro Fortaleza Formation deposits have been incorrectly referred to the Pari Aike Formation[4,7-9] or the Mata Amarilla Formation[10]. Although there is some uncertainty regarding the chronostratigraphic age of the Cerro Fortaleza Formation[6], it is most commonly assigned to the Campanian–Maastrichtian stages of the Upper Cretaceous because it overlies paralic and nearshore marine deposits of the La Anita Formation[3-5] that contain Campanian invertebrate assemblages[3,4,6,11]. However, more work (particularly radiometric dating, non-vertebrate biostratigraphy, and magnetostratigraphy) is necessary to refine the ages and stratigraphic relationships of the Upper Cretaceous series in this region.

Three fluvial facies comprise the bulk of the Cerro Fortaleza Formation: channel fill, crevasse splay, and floodplain. The channel fill facies range from trough cross-stratified coarse to medium sandstone, to cross-bedded to planar very fine sandstone, to mudstone. Splay deposits are common and often display syndepositional deformation at their base. Avulsion surfaces possibly resulting from crevasse splay formation, histosols[10], carbonaceous root fossils, and abundant silicified wood[6] all indicate a poorly drained, low-lying, forested terrain.

A fortuitous taphonomic setting led to the extraordinary completeness of the *Dreadnoughtus schrani* holotype (MPM-PV 1156). Fossil skeletons of large-bodied sauropod dinosaurs are typically fragmentary, in part because rapid peri- and/or post-mortem burial is necessary to preserve articulated or closely associated skeletal segments[12]. Given the considerable body volume of large sauropods, it is unlikely for any particular individual to have perished in a depositional setting capable of rapidly entombing its carcass. An exception to this scenario may pertain to large individuals that are buried in overbank deposits, such as crevasse splays, which are associated with a relatively high preservation potential[13-16].

The *Dreadnoughtus* individuals MPM-PV 1156 and MPM-PV 3546 were found in deposits that we interpret as a crevasse splay, consisting of a mixed lithosome of sandstone with small-scale cross-bedding and scour-and-fill structures, and mudstone with allochthonous plant remains. Bundles of these units were distorted into convoluted bedforms, which indicate the rapid emplacement, liquefaction, and penecontemporaneous deformation of these deposits. During the liquefaction phase, reduced shear strength of the substrate caused the subsidence of the carcasses of both individuals. Many elements from each partial skeleton were preserved with a steeply inclined attitude, extreme examples being the pubis, ischium, and femur of the paratype (MPM-PV 3546), which came to rest in a vertical orientation. The extraordinary completeness of the holotype can be attributed to a combination of rapid sedimentation and subsidence during peri- and/or post-mortem burial.

The preservation of mostly left-handed appendicular elements indicates that the holotypic *Dreadnoughtus* individual (MPM-PV 1156) probably came to rest on its left side. Many of the right-handed elements were either displaced before burial or eroded prior to discovery. The slightly smaller, paratypic *Dreadnoughtus* (MPM-PV 3546) was discovered on the eroding flank of the promontory that contained both individuals. Additional portions of the paratype, if initially preserved, are likely to have been destroyed by erosion associated with the retreat of the hillside. The shed crowns of several theropod teeth (probably referable to the megaraptoran tetanuran *Orkoraptor burkei*[17])—together with probable tooth marks on a caudal vertebra of the paratype (Supplementary Fig. 8A) and the centrum of a dorsal vertebra that could belong to either individual (Supplementary Fig. 8B)—suggest that perimortem scavenging may have removed portions of MPM-PV 3546, and possibly parts of MPM-PV 1156 as well.

3. Material preserved

Detailed descriptions and comparisons of all known *Dreadnoughtus* skeletal elements are currently in progress. Here we provide a preliminary overview of some of the most salient aspects of the osteology of this titanosaur.

Craniomandibular skeleton and dentition. The *Dreadnoughtus schrani* holotype (MPM-PV 1156) includes a small fragment of a dentigerous cranial bone, probably a maxilla, that is broken into two pieces. The element is mediolaterally compressed and its medial surface is poorly preserved. The ventral (i.e., occlusal) surface of the larger piece (Supplementary Fig. 2A) is partly intact, and preserves the remnants of approximately five alveoli that are of appropriate size and morphology to have housed the single sauropod tooth known from the *Dreadnoughtus* quarry (Supplementary Fig. 2B). Found approximately 50 cm from the maxilla fragment, this tooth is 3.5 cm in preserved length and exhibits the narrow-crowned, chisel-like shape typical of derived titanosaurians (e.g., *Antarctosaurus wichmannianus*, *Bonitasaura*, *Brasilotitan*, *Maxakalisaurus*, *Nemegtosaurus*, *Rapetosaurus*, *Rinconsaurus*, *Tapuiasaurus*). It is oval in cross section, slightly broader mesiodistally than labiolingually. One face, presumably the labial, is slightly convex, whereas the opposite (lingual) side is flat. The crown is marked by a planar, high-angled wear facet on the apex of its presumed lingual face, as well as a thin, longitudinal facet along either its mesial or distal margin.

Postcranial axial skeleton. A very large (centrum length = 1.13 m), nearly complete posterior cervical vertebra (approximately the ninth) and part of a smaller, more anterior cervical vertebra were recovered from the *Dreadnoughtus* type locality. Based on its position in the quarry, the more anterior cervical vertebra may pertain to the paratypic specimen MPM-PV 3546, although the possibility that it is instead part of the holotype (MPM-PV 1156) cannot be completely ruled out. The posterior ~half of its opisthocoelous centrum lacks lateral pneumatic fossae ('pleurocoels'). The ventrolateral edge of the centrum is comprised by the well-developed posterior centroparapophyseal lamina, whereas the dorsolateral edge is formed by the posterior centrodiapophyseal lamina. On the neural arch, the postzygodiapophyseal lamina angles steeply anteroventrally toward the missing diapophysis.

The enormous posterior cervical vertebra of MPM-PV 1156 (Fig. 1A–D, Supplementary Figs. 3, 10) is missing only the right diapophysis, the left prezygapophysis, and the posterior end of the right postzygapophysis. The vertebra is somewhat deformed, with most right lateral structures having been shifted dorsally and left lateral structures ventrally. Several specific taphonomic alterations are observed. The neural spine has been bowed to the right, rendering its right side concave and its left side convex. This compression of structures towards the right side of the element has elongated the corresponding areas of the left side, increasing the distance between the left diapophysis and the neural spine. The right spinoprezygapophyseal lamina has been broken in two; its pieces are offset and shifted dorsoventrally with respect to one another, resulting in an overlap of 10 cm. Additionally, an angular bend has formed on the ventral surface, and extends asymmetrically under the right parapophysis.

Multiple breaks reveal that the interior of the vertebra is comprised entirely of camellate tissue. Its centrum is strongly opisthocoelous. Though deformation has altered the shape of both of its articular surfaces, their original morphology is discernible. The anterior condyle is dorsoventrally compressed, being much wider than tall, whereas the posterior cotyle is ovate in posterior view. The taphonomic displacement of the parapophyses has exaggerated the concavity

of the ventral surface of the centrum. Nevertheless, this surface was at least slightly concave throughout most of its length, becoming convex only at its posterior extreme.

As is the case in the more anterior cervical vertebra, the lateral surface of the centrum is framed by the posterior centroparapophyseal and posterior centrodiapophyseal laminae. It is deeply concave anteriorly, between the parapophysis and diapophysis, and gradually shallows posteriorly as these laminae grade into the centrum. Although well-developed pneumatic fossae are absent on both lateral surfaces, these surfaces bear a crenulated texture indicative of contact with soft-tissues, probably pneumatic diverticula[18-21]. This texture is particularly distinct anteriorly. Additionally, there are multiple irregular openings along the damaged margin of the right posterior centrodiapophyseal lamina, in the area of the missing diapophysis. It is unclear whether these would have opened onto the lateral surface of the vertebra in life, or if they are pneumatic cavities internal to the diapophysis that were exposed by the loss of this structure.

The parapophyses extend ventrolaterally from the centrum and are restricted to its anterior one-third. In lateral view, the posterior centroparapophyseal laminae form a smoothly concave arc from the parapophyses to the centrum, and continue as distinct ridges to the posterior cotyle of the latter. Whereas the left parapophysis is dorsoventrally flattened and rounded in dorsolateral view, the right parapophysis has a dorsally-deflected flange that would have articulated with the missing cervical rib.

The neural arch is relatively low, with a height (85 cm) that is lower than the centrum is long (113 cm, including the anterior articular condyle). The left diapophysis is similar to the parapophyses in being flattened, rounded, and anteriorly restricted. The posterior centrodiapophyseal lamina links the diapophysis with the centrum but disappears before reaching the posterior cotyle; its lateral margin is straight in dorsal view. The postzygodiapophyseal lamina is posterodorsally directed and deeply concave in dorsal view. Together, the posterior centrodiapophyseal and postzygodiapophyseal laminae enclose the deep, triangular postzygapophyseal centrodiapophyseal fossa. The left postzygapophyseal centrodiapophyseal fossa does not appear to be perforated by foramina. However, the smooth, crenulated texture of its walls suggests that, in life, it was probably in contact with pneumatic diverticula. Unfortunately, it is not possible to completely remove sediment from the deepest part of the fossa, where foramina are most likely to be present. Additionally, the right postzygapophyseal centrodiapophyseal fossa appears to have irregular openings into the interior of the bone, near the junction of the posterior centrodiapophyseal and postzygodiapophyseal laminae. It is not clear if these are pneumatic openings or internal cavities.

The right prezygapophysis extends far beyond the anterior margin of the anterior articular condyle of the centrum. The spinoprezygapophyseal lamina remains well developed to the anterior tip of the prezygapophysis, laterally bounding its articular facet, which is flat. The centroprezygapophyseal lamina is robust and undivided. The postzygapophyses do not surpass the posterior margin of the centrum. Their articular surfaces are flat and triangular. Together with the intrapostzygapophyseal lamina, the short, robust centropostzygapophyseal laminae delimit the heart-shaped neural canal posteriorly. Although the neural canal has been taphonomically distorted, its dorsal margin appears to have been flatter than its rounded ventral margin.

The neural spine is formed by the spinoprezygapophyseal and spinopostzygapophyseal laminae, which meet at a nearly right angle (~80°). The spine is robust and projects directly dorsally, forming a triangular, pointed apex just anterior to the anteroposterior midline of the

centrum. In lateral view, the spinoprezygapophyseal lamina is straight, extending posterodorsally from the prezygapophysis at an approximate 45° angle. The right spinoprezygapophyseal lamina appears strongly curved in lateral view, but this is an artefact caused by the breakage and subsequent offset and overlap of this lamina, which has taphonomically shortened the distance between the neural spine and the prezygapophysis on this side. The posterior margins of both spinopostzygapophyseal laminae are incomplete. Despite this, enough of these laminae are present to indicate that they were gently concave in lateral view.

The spinodiapophyseal fossae are distorted. The less deformed left fossa is broad, encompassing the majority of the lateral side of the neural spine. It tapers to a deep, narrow depression on the spine, immediately dorsal to the posterior extremity of the diapophysis. Though the surface bone within the spinodiapophyseal fossa is not intact, the dorsal surface of the diapophysis has the smooth texture suggestive of contact with pneumatic soft-tissues. The neural spine is transversely narrow, with none of the lateral expansions or laminae seen in some other titanosaurs (e.g., *Mendozasaurus*, *Puertasaurus*, *Futalognkosaurus*)[22-24].

Prespinal and postspinal laminae are absent. The spinoprezygapophyseal laminae coalesce on the anterior face of the neural spine, at a point approximately two-thirds the dorsoventral height of the spine. Ventral to this point, these laminae dorsolaterally bound the deep, triangular spinoprezygapophyseal fossa, which is floored by the remnants of the broken intraprezygapophyseal lamina. The spinopostzygapophyseal laminae remain separate until the very tip of the posterior face of the spine. With the intrapostzygapophyseal lamina, these laminae delimit the extremely deep spinopostzygapophyseal fossa, which is triangular at its posterior margin but becomes more ellipsoid the deeper it penetrates into the spine. Collectively, the exceptionally deep spinoprezygapophyseal and spinopostzygapophyseal fossae and the triangular lateral profile of the neural spine lend the spine a conformation resembling an A-frame tent.

In sauropod cervical vertebral sequences, the neural spines generally become dorsoventrally taller and anteroposteriorly narrower as one moves posteriorly through the series, whereas the centra become shorter and deeper[25]. Consequently, the substantial height and acuteness of the neural spine of the large MPM-PV 1156 cervical vertebra indicates that it does not pertain to the anterior part of the series. This is further supported by the large size of the vertebra, because sauropod cervical vertebrae gradually become larger towards the base of the neck. Nevertheless, the centrum is elongate (Elongation Index[26] = 3.06), indicating that the vertebra is not one of the posterior-most cervical vertebrae either. In sauropods, the longest cervical centra are typically positioned in the middle of the neck. Accordingly, we hypothesize that this MPM-PV 1156 vertebra is a mid-posterior cervical vertebra, probably occupying approximately position nine.

Two cylindrical fragments of ossified tissue were found draped across this vertebra, whereas a third fragment extended anteriorly past the centrum. The first is a long (> 65 cm) fragment that lies atop the dorsal surface of the left parapophysis and extends posterodorsally to contact the centrum at the posterior end of the posterior centrodiapophyseal lamina. It is ellipsoid in cross section, tapering from a width of 2.5 cm over the parapophysis to 1.5 cm where it contacts the posterior centrodiapophyseal lamina. The second fragment, 22 cm in length, originates ventral to the medial edge of the left postzygapophysis before curving dorsolaterally towards the right spinopostzygapophyseal lamina. It is also ellipsoid in cross section, and tapers from a width of 1.4 cm beneath the postzygapophysis to 1.1 cm at the point it terminates in a broken end in the spinopostzygapophyseal fossa. The third fragment is ~51 cm long and ellipsoid

in cross section, with a maximum width of 2.8 cm. As seen in thin section (Supplementary Fig. 4), this structure is composed predominantly of secondary osteons, although primary tissue is visible interstitially and near the outer margin. This primary tissue consists of mineralized collagen fibril bundles, which indicates that the structure is an ossified tendon and not periosteal bone.

Due to the angles at which these fragments originate and terminate with respect to one another, their similar cross-sectional shape, and the gradual tapering observed within and between the pieces, we consider it likely that these three fragments were originally part of a single long structure that was pressed against the left side of the centrum after death and subsequently wrapped around the left postzygapophysis. Like these fragments, the posterior processes of elongate sauropod cervical ribs are ellipsoid in cross section. Moreover, the histology of these processes indicates that they are composed of ossified tendon rather than periosteal bone[27,28]. Thus, the tendon fragments recovered with the large MPM-PV 1156 cervical vertebra probably represent parts of the posterior process of a single rib from a more anterior vertebra in the series. When the total length of the incomplete fragments (> 138 cm) is compared to the centrum length of the preserved vertebra, these data suggest that *Dreadnoughtus* possessed elongate cervical ribs that may have extended half a centrum length or more past the posterior end of the vertebra to which they were attached.

Eight partial to nearly complete dorsal vertebrae (Fig. 1E–J, Supplementary Figs. 5, 11, 12) and numerous dorsal ribs (Supplementary Fig. 6A) were recovered from the *Dreadnoughtus* type locality. Based on their positions in the quarry, some of these elements are undoubtedly part of the holotype (MPM-PV 1156); the assignment of other dorsal vertebrae and ribs is less certain, and some may belong to the paratype (MPM-PV 3546). All dorsal centra are internally comprised of camellate tissue, and are strongly opisthocoelous with elliptical, well-developed lateral pneumatic fossae. Most centra are considerably wider than tall, though in some cases their width has been exaggerated by taphonomic compression. Neural arch pedicels (i.e., the part of the neural arch ventral to the zygodiapophyseal table) are low, and transverse processes are directed laterally or slightly anterolaterally. Neural spines are as tall or taller than their corresponding neural arch pedicels and oriented posterodorsally.

The most anteriorly-positioned dorsal vertebra (Fig. 1E, Supplementary Figs. 5A, 11) pertains to the anterior part of the series; it is virtually complete but severely dorsoventrally compressed. The neural arch is anteriorly placed, such that its anterior edge is nearly flush with that of the centrum, but its posterior edge is inset. Unlike the condition in more posterior dorsal vertebrae, spinoprezygapophyseal laminae are present; short and thin, they merge with the prespinal lamina approximately 4 cm dorsal to the base of the neural spine. A middle dorsal vertebra (Supplementary Fig. 8B) is incomplete and laterally crushed. Its left side is mostly intact but is missing the lateral extremes of the parapophysis and diapophysis. A second middle dorsal vertebra (Fig. 1F–G, Supplementary Fig. 5B–C) definitively pertains to the holotype; it is mostly complete but anteroposteriorly compressed.

Several posterior dorsal vertebrae are also preserved, two of which are nearly complete and largely undistorted. In the first of these (Fig. 1H, Supplementary Fig. 5D), the lateral pneumatic fossae of the centrum are anteriorly positioned, and the posterior centrodiapophyseal fossae are relatively deeper than in many of the other vertebrae. In the second vertebra (Fig. 1I–J, Supplementary Figs. 5E–F, 12), the neural spine is more vertical, and a short lamina, probably the posterior centroparapophyseal lamina, extends from the intersection of the posterior

centrodiapophyseal and accessory posterior centrodiapophyseal laminae to the parapophysis. This presumed posterior centroparapophyseal lamina transects the large parapophyseal centrodiapophyseal fossa. The prespinal lamina is faint ventrally but becomes more prominent dorsally; nevertheless, it may not reach the apex of the neural spine.

In both of these posterior dorsal vertebrae, and in contrast to the condition in more anterior dorsal vertebrae, the spinodiapophyseal lamina bifurcates into anterior and posterior branches that collectively enclose a coel (the spinodiapophyseal lamina fossa). A similarly bifid spinodiapophyseal lamina also occurs in a neural arch fragment that is interpreted as that of another posterior dorsal vertebra. The posterior ramus of the spinodiapophyseal lamina merges with the spinopostzygapophyseal lamina at a rugose tuberosity, presumably indicative of soft-tissue attachment, that is subtriangular in anterior and posterior views but ovate in lateral view. Furthermore, the dorsal surface of each posterior dorsal transverse process is marked by a well-defined, semi-circular area of mediolaterally-oriented ridges and grooves, also probably for soft-tissue attachment. A comparable condition may be present on the left transverse process of the middle dorsal vertebra of the holotype mentioned above (Fig. 1F–G, Supplementary Fig. 5B–C), but the strong anteroposterior compression of this vertebra renders this difficult to confirm. If this grooved area is indeed present on this middle dorsal vertebra, it is more medially placed than in the posterior dorsal vertebrae.

Two other posterior dorsal vertebrae are poorly preserved, lacking much of the neural arch. Both exhibit what are probably posterior centroparapophyseal laminae. One of them, the posterior-most dorsal vertebra known for *Dreadnoughtus*, belongs to the holotype. The lateral pneumatic fossae of the centrum are anteriorly placed, and there is a thin vertical lamina on the posteroventral part of the neural arch, between the neural canal and the area of the missing intrapostzygapophyseal lamina.

Portions of numerous dorsal ribs are preserved, including at least four to six nearly complete ribs (Supplementary Fig. 6A). At least four of these exceed 2 m in length. Pneumatopores are clearly present near the heads of two ribs, indicating that at least some of these bones were pneumatized. Furthermore, pneumatic cavities occur in the proximal shafts of several ribs. Cross-sectional shape varies between ribs as well as along the length of a single rib. Proximally, near the head, the ribs are triangular to semilunate in cross section, and become more plank-like towards the distal end.

The partially preserved sacrum of the *Dreadnoughtus schrani* holotype (MPM-PV 1156) (Fig. 1K, Supplementary Fig. 13) consists of at least four (probably more) coossified vertebrae that represent at least the third through sixth sacral vertebrae. The ventral surface is well preserved, but most of the dorsal surface, including the neural arches, is missing. Breaks that expose the interior of the sacrum reveal a camellate morphology, indicating that at least some of the centra and ribs were pneumatized. The last sacral centrum is much wider than tall and posteriorly concave to articulate with the anterior face of the biconvex first caudal vertebra. The left sacral ribs are missing, although two isolated ribs were recovered and likely belong to this individual. Three right sacral ribs are well preserved but dorsoventrally crushed. The ?second and ?fourth ribs are oriented slightly posterolaterally, whereas the sixth projects strongly anterolaterally. The distal margins of the articulated sacral ribs widen and fuse to form a sacricostal yoke. Ventral intercostal foramina are present between the sacral ribs, but there is no indication of transverse foramina. Between the three intact sacral ribs, two broken knobs emanate from the right lateral face of the coossified centra; we suspect these may be the bases of

the third and fifth sacral ribs, respectively. The sacrum of the paratype (MPM-PV 3546) is strongly taphonomically compressed in an anteroposterior direction but preserves all six centra. The first sacral vertebra has a convex anterior face, whereas the sixth sacral vertebra possesses a concave posterior face as in the sacrum of the holotype. The dorsal surface of the fused centra is not preserved although the entire posterior face of the last centrum is present. In the paratype, the partially preserved fifth sacral rib appears narrower and less robust than the sixth, lending support to our identification of the more posteriorly-positioned knob on the right side of the holotypic sacrum as the base of the fifth rib.

The caudal sequence of *Dreadnoughtus* is nearly completely known, missing only a few posterior vertebrae and approximately three posterior haemal arches (Fig. 1L–M, Supplementary Figs. 6B–G, 7, 14). In overall morphology, the vertebrae closely resemble those of representatives of the lithostrotian subclade Aeolosaurini (e.g., *Aeolosaurus*, *Gondwanatitan*) as well as a few other South American titanosaurs such as *Adamantisaurus*, *Baurutitan*, *Pellegrinisaurus*, and *Trigonosaurus*. Represented in the holotype, the first caudal vertebra is biconvex, as in several lithostrotians (e.g., *Alamosaurus*, *Baurutitan*, *Pellegrinisaurus*[29,30]). Only the centrum, the left transverse process, and a small part of the right transverse process are preserved; the entirety of the neural arch is missing. The centrum has been deformed, such that its articular faces are offset from one another. The anterior face, though still convex, is flatter than the posterior face; the latter is strongly convex to articulate with the deeply concave anterior face of the second caudal centrum. The lateral faces of the first caudal centrum are concave. The centrum exhibits a distinct sagittal keel ventrally, such that it is nearly V-shaped in cross section at its anteroposterior midline. Among titanosaurs, this feature is otherwise known only in the single preserved anterior caudal vertebra of the possible saltasaurine *Bonatitan*[31]. Because this taxon is not thought to be closely related to *Dreadnoughtus*, and because this *Bonatitan* vertebra is probably not the first caudal vertebra, we regard a ventral keel on the first caudal centrum as an autapomorphy of *Dreadnoughtus*. The left transverse process of the *Dreadnoughtus* first caudal vertebra is much larger and more robust than those of more posterior caudal vertebrae, occupying most of the dorsoventral extent of the centrum. A rugose tuberosity is present on the dorsal portion of the posterior side of the process. Comparable, though possibly not identical, conditions occur in the first caudal vertebra of *Epachthosaurus*[32] and *Saltasaurus*[33,34] and in anterior caudal vertebrae of *Trigonosaurus*[35].

Posterior to the first caudal vertebra, the centra are strongly procoelous with deeply concave anterior articular cotyles and strongly convex posterior condyles. In the anterior caudal vertebrae, the anterior faces of the centra are taller than wide and subcircular in contour, and the posterior condyles are dorsally displaced. The tall lateral faces are anteroposteriorly concave and exhibit marked rugosities, particularly toward their anterior and posterior margins. There are no pneumatic fossae, but as in several other titanosaurs (e.g., *Adamantisaurus*, *Alamosaurus*, *Paralititan*, *Pellegrinisaurus*) small foramina pierce the lateral surfaces of several of the centra ventral to the transverse processes. The ventral surfaces possess a deep, well-defined groove. The transverse processes are short, robust, and posterolaterally oriented, and persist posteriorly until the 12th caudal vertebra. The neural arches are placed over the anterior half of the centrum, close to its anterior margin. The robust prezygapophyses are slightly anterodorsally directed and their lateral faces are gently convex. The prezygapophyseal articular facets are subcircular in contour. The postzygapophyses are weakly developed and recessed; as a result, they are V-shaped in posterior view. Their articular facets are small, dorsoventrally oriented, and subcircular in outline. Most anterior caudal neural spines are gently posteriorly oriented but with anteriorly-

directed apices, and all possess strongly developed prespinal and postspinal laminae; these are especially pronounced in the anterior-most vertebrae, to a degree that is greater than in other titanosaurs. The neural spines are wider anteroposteriorly than transversely, and their lateral surfaces are crossed by spinoprezygapophyseal and spinopostzygapophyseal laminae. As in anterior caudal vertebrae of several other titanosaurs, including *Adamantisaurus*[36], *Alamosaurus*[37], *Bonatitan*[31], and *Mendozasaurus*[38], these laminae frame a pneumatocoel that occupies the position of the confluent postzygapophyseal spinodiapophyseal/postzygapophyseal centrodiapophyseal fossa of Wilson et al.[39] Nevertheless, the morphology of this structure in *Dreadnoughtus* differs from that in other taxa in being extensively subdivided into a complex array of pneumatic openings.

Compared with more anterior caudal vertebrae, the centra of the middle caudal vertebrae have a more centrally placed posterior condyle and dorsoventrally lower, anteroposteriorly flatter lateral sides. As a result, the centra are subquadrangular in lateral view. The rugosities observed in the anterior caudal centra are also present in the middle caudal centra. Moreover, a marked sagittal groove divides the haemal arch facets on the ventral surface, and a longitudinal ridge adorns the lateral aspect of the neural arch base. The neural arches are placed over the anterior half of the centrum; however, in the anterior-most section of the middle caudal sequence, they are near the anterior border, whereas they are situated slightly more posteriorly through the remainder of the sequence. The prezygapophyses are anteriorly projected and strikingly elongate, extending more than half the lengths of their respective centra. As in the anterior caudal vertebrae, the postzygapophyses of the anterior-most middle caudal vertebrae are weakly developed and sunken, whereas in the remainder of the middle caudal sequence they migrate to the posteroventral border of the neural spine. The neural spines are plate-like, much wider anteroposteriorly than transversely. In the anterior-most middle caudal vertebrae (positions 11 to 13), the anterodorsal border of the neural spine is sharply pointed and anteriorly projected, extending well beyond the anterior margin of the centrum, a condition that is not seen in other titanosaurs. The neural spines of the 15th through 18th vertebrae are subvertical, whereas those of caudal vertebrae 19 to 22 are posterodorsally oriented.

The posterior caudal vertebrae were found in close proximity to the articulated caudal sequence of the holotype, and continue this series either without interruption or with only one vertebra missing in between. The posterior centra are relatively anteroposteriorly elongate in comparison to those of more anterior vertebrae, and their posterior articular condyles are centrally located. Their lateral surfaces are gently concave, and a shallow groove occurs on the ventral face. The neural arches are placed over the anterior half of the centrum, but slightly posteriorly removed from its anterior margin. The long, slender prezygapophyses surpass the anterior margin of the centrum, whereas the postzygapophyses are situated near the posterior edge and have subcircular articular facets. The low, plate-like neural spines show no evidence of laminae.

A total of 23 haemal arches were recovered from the *Dreadnoughtus* quarry. Fifteen were attached to the articulated series of anterior and middle caudal vertebrae (caudal vertebrae 5 to 21) of MPM-PV 1156, so their positions in the tail are known with certainty. The remaining eight haemal arches were disarticulated. Five of these duplicate positions already represented in the articulated caudal series, and therefore belong to the paratype, MPM-PV 3546. The remaining three anterior haemal arches were associated with the anterior-most caudal vertebrae of MPM-PV 1156, and thus presumably represent the anterior-most haemal arches in the tail.

These three haemal arches progressively lengthen from anterior to posterior, with the third being the longest in the caudal series. The first haemal arch is relatively slender, though this feature is accentuated by anteroposterior taphonomic compression. All of the articulated haemal arches are generally well preserved and dorsally open; however, some are incomplete or taphonomically deformed. Anterior haemal arches are Y-shaped in anterior and posterior views, with a haemal canal that occupies approximately half the length of the bone. The facets for articulation with the caudal centra are well-marked and subcircular in outline. They are not divided into 'double articular facets' as in *Aeolosaurus*[40]. The distal blade is remarkably anteroposteriorly expanded, rendering it paddle-shaped in lateral view, more so than in any other titanosaur. The robust posterior haemal arches are V-shaped in anterior view, with a haemal canal that spans more than 70% the length of the bone.

Appendicular skeleton. We describe the scapula in anatomical orientation, as presented in Fig. 2 of our main text, with the scapular blade inclined at approximately 50° from the horizontal. In *Dreadnoughtus* (MPM-PV 1156), the acromion and acromial ridge of the scapula are well developed, and the posterodorsal end of the scapular blade is only slightly expanded. As in *Elaltitan*, *Mendozasaurus*, *Paralititan*, and several non-titanosaurian titanosauriforms, there is a single, well-developed ventromedial tubercle. An oblique ridge that is not observed in other titanosaurs extends along the medial surface from the posteroventral margin proximally to the anterodorsal margin distally, posterior to the M. subscapularis attachment. The dorsolateral part of the coracoid has a well-developed M. biceps brachii scar, as in *Rapetosaurus*[41]. The coracoid foramen passes obliquely through the bone, from the centre of the lateral face to the scapular articulation medially, unlike any other titanosaur. Martin[42] and Wilhite[43] have proposed that, during sauropod ontogeny, the coracoid foramen migrates anteriorly from the scapula–coracoid articulation into the coracoid body; consequently, the distinctive morphology of the MPM-PV 1156 coracoid may be due to the osteological immaturity of this individual. The proximomedial process of the humerus is less developed and medially projected than in many titanosaurs (e.g., *Gondwanatitan*[44], *Paralititan*[45], *Malawisaurus*[46]). The *Dreadnoughtus* ulna exhibits a prominent muscle scar roughly one-quarter of the way down the anterior face, as in *Aeolosaurus* sp.[47] and *Neuquensaurus*. The distal end of the ulna is mediolaterally expanded as in *Pitekunsaurus*[48], *Alamosaurus*, and *Opisthocoelicaudia*. The distal radius is nearly square in distal view, with subequal mediolateral and anteroposterior dimensions. This shape contrasts with the mediolaterally expanded (e.g., *Neuquensaurus*, *Tapuiasaurus*, *Alamosaurus*, *Opisthocoelicaudia*) or oval (e.g., *Rapetosaurus*, *Saltasaurus*) distal radii of other titanosaurs, and apparently represents a reversal to the ancestral sauropod state[49]. This feature is therefore proposed as a local autapomorphy of *Dreadnoughtus*. Another diagnostic character of the new titanosaur is a well-developed depression on the posteromedial surface of the proximal radius.

All four ilia, from both specimens, lack their posterodorsal margins and much of their postacetabular processes. Their pubic and ischial peduncles are mediolaterally broad, and the latter is not confluent with the postacetabular process, unlike in saltasaurines. The pubes are twisted in a fashion similar to that seen in *Saltasaurus*. A weak ventrolateral longitudinal ridge is present, as in *Aeolosaurus* and *Futalognkosaurus*, but it is not as strongly developed as in *Saltasaurus* or *Uberabatitan*. The ischia have mediolaterally wide and laterally arched pubic articular surfaces, as in *Aeolosaurus* sp.[46]. The distal condyles of the femur are not expanded anteriorly so as to be visible in anterior view (thus lacking this proposed synapomorphy of Saltasaurinae[37]), are roughly equal in breadth, and are taphonomically compressed to an anterolateral angle of 50° to 60°. The proximal and distal ends of the right tibia are expanded, but

are rotated only about 30° relative to one another due to taphonomic compression. The distal fibula possesses a strong medial lip for articulation with the astragalar ascending process, as seen in saltasaurines and incipiently in *Antarctosaurus wichmannianus*[50]. The astragalus tapers medially, is proximally flat and distally convex, and has a short ascending process. Metatarsals I and II are robust with subequal distal condyles separated posteriorly by shallow flexor depressions, a morphology that accords with hypotheses of pedal phalangeal motion in titanosaurs[41]. The ungual of pedal digit I is mediolaterally narrow and sickle-shaped as in essentially all other sauropods[36,49].

4. Digital reconstruction

To better visualize and document the skeletal morphology of *Dreadnoughtus schrani*, we gathered high-resolution, three-dimensional laser scans of all known elements of the holotypic and paratypic specimens (with the exception of selected cervical and dorsal rib fragments) using a NextEngine Model 2020i Desktop 3D Laser Scanner. We produced three-dimensional digital models of all scanned elements using NextEngine ScanStudio HD PRO software, and articulated these models in likely anatomical positions using Autodesk Maya 3D animation software. We then used GeoMagic Studio software to export all components of the digital skeleton as a series of ten three-dimensional Adobe Portable Document Format (PDF) files (see Supplementary Figs. 9–18). (Viewing and navigating Adobe 3D PDF files requires Adobe Acrobat or Acrobat Reader. The latter is freely available for download at http://get.adobe.com/reader/.) Each 3D PDF depicts a different component of the *Dreadnoughtus* skeleton. Users may rotate each component into whatever orientation they prefer; moreover, in each file, each bone is placed on an individual layer, such that, if they wish, users may view only a certain bone or bones. (As an example, if a user wished to examine the anterior articular cotyle of the tenth caudal vertebra, which is obscured by more anterior vertebrae in the articulated model, they could 'turn off' all elements anterior to this bone and then manipulate it into anterior view.)

The resulting digital reconstruction (a 'virtual mount') provides considerable insight into the morphology of *Dreadnoughtus* in particular and gigantic titanosaurs more generally. Assembling the actual bones into a physical mounted skeleton would be physically, technically, and financially challenging, and would risk damage to the fossils. Compounding these liabilities, mounted specimens can be difficult to disarticulate for further examination, which can deter future study. In a virtual environment, fossil bones weighing hundreds of kilograms can be manipulated with ease, thus facilitating the testing of anatomical and biomechanical hypotheses. For example, to ascertain whether the enigmatic biconvex vertebra (Fig. 1L–M, Supplementary Fig. 7) represents an unfused seventh sacral vertebra, as in the saltasaurine *Neuquensaurus*[29,51], or, alternatively, the first vertebra in the caudal series, we virtually articulated the sacral and anterior caudal region of *Dreadnoughtus*. Doing so revealed that the transverse processes that extend laterally from the biconvex vertebra are too short to have articulated with the ilia (Supplementary Fig. 9). We therefore interpret this vertebra as the first caudal vertebra. Additionally, most *Dreadnoughtus* bones exhibit well-defined scars that indicate muscle, tendon, and ligament attachments. In-progress work entails the use of digital models and 3D printed replicas of bones to provide scaffolding for the reconstruction of soft-tissues and for the evaluation of biomechanical hypotheses via virtual and robotic models (e.g., Voegele et al.[52]).

5. Comparison with *Puertasaurus*

Puertasaurus reuili is another very large titanosaur from south-western Santa Cruz Province, collected from an exposure of the Cerro Fortaleza Formation approximately 13 km northwest of the *Dreadnoughtus schrani* site[23]. The chronostratigraphic range of the 350 m-thick Cerro Fortaleza Formation is contentious and poorly constrained[6], as are correlations between its many discontinuous outcrops. Given the uncertain stratigraphic relationships of the *Dreadnoughtus* and *Puertasaurus* localities, it is unclear whether these taxa were coeval, and indeed, it is possible that they may have been temporally separated by hundreds of thousands of years or more. Coupled with our lack of knowledge of the geographic ranges of these taxa, this renders premature any consideration of the possible occurrence and implications of sympatric or parapatric distributions for these two giant sauropods.

Regrettably, because the type and only known specimen of *Puertasaurus* (MPM-10002) consists of four bones (one posterior cervical, one anterior dorsal, and two incomplete caudal vertebrae), extensive comparisons with *Dreadnoughtus schrani* are not possible. Nevertheless, the single known posterior cervical vertebra of *Puertasaurus* (regarded by Novas et al.[23] as the ninth) occupies at least approximately the same serial position as does the nearly complete cervical vertebra of MPM-PV 1156 (identified as approximately the ninth herein). Although the *Puertasaurus* cervical vertebra is incomplete posteriorly and dorsally, enough of it is preserved to enable the assessment of multiple aspects of its original morphology. Hence, some comparisons between these taxa may be made on the basis of this part of the skeleton.

The most striking difference between the posterior cervical vertebrae of *Dreadnoughtus* and *Puertasaurus* is the morphology of their neural spines. Although only partially preserved, the neural spine of *Puertasaurus* is complete enough to demonstrate that it was remarkably transversely expanded. Indeed, the broadly laterally expanded spine of *Puertasaurus* has been regarded as a diagnostic feature of this titanosaur[23]. This expansion arises from a substantial transverse thickening of the dorsal part of the spine, without the participation of spinoprezygapophyseal or spinopostzygapophyseal laminae[53]. Remarkably, as a result of this lateral expansion, the transverse width of the posterior cervical neural spine of *Puertasaurus* is estimated to have exceeded that of the centrum[23]; indeed, with the possible exception of *Mendozasaurus*[22], *Puertasaurus* has the proportionally widest cervical neural spine known in any titanosaur. In the *Dreadnoughtus* cervical vertebra, by contrast, the presence of spinodiapophyseal fossae renders the lateral aspect of the neural spine gently concave, and there is no evidence of the lateral expansion that is diagnostic of *Puertasaurus*.

Furthermore, the shape and length of the spinoprezygapophyseal lamina differs between *Dreadnoughtus* and *Puertasaurus*. In MPM-PV 1156, the pronounced spinoprezygapophyseal lamina originates at the anterior extreme of the prezygapophysis and rapidly angles steeply posterodorsally. This results in a tall, dorsally pointed neural spine with its apex positioned immediately anterior to the anteroposterior midline of the vertebra. In *Puertasaurus*, conversely, the neural spine apex is situated posterior to the midline, and the spinoprezygapophyseal lamina is indistinct on the dorsal surface of the prezygapophysis. Instead, this lamina rises gradually from the posterior end of the prezygapophysis, forming a low angle with the base of the neural arch. Additionally, in *Puertasaurus*, the spinoprezygapophyseal laminae do not meet on the sagittal midline, but instead merge with the laterally expanded neural spine; as a result, the spinoprezygapophyseal fossa is transversely broad and dorsally open. In *Dreadnoughtus*, by

contrast, the spinoprezygapophyseal laminae fuse approximately two-thirds of the way up the neural spine, dorsally bounding the deep, triangular spinoprezygapophyseal fossa.

The serial positions of these *Puertasaurus* and *Dreadnoughtus* cervical vertebrae cannot be determined without some degree of uncertainty; nevertheless, based on comparisons with complete and nearly complete titanosaurian necks (e.g., those of *Futalognkosaurus*[24], *Rapetosaurus*[41], and the unidentified Brazilian titanosaur 'Peirópolis Series A'[34]), these vertebrae are likely within one position of each other, and may even occupy the same position. The degree of morphological change that would be required to transform the *Dreadnoughtus* posterior cervical vertebra into that of *Puertasaurus* over one or even two serial positions is not known in any titanosaur. It is therefore highly unlikely that the differences observed between the posterior cervical neural spines of MPM-PV 1156 and *Puertasaurus* are the result of positional variation.

Novas et al.[22] described the single preserved dorsal vertebra of *Puertasaurus* as the second within the series. In all of the eight known dorsal vertebrae of *Dreadnoughtus*, the parapophyses are situated on the neural arch, indicating that these vertebrae occupy a more posterior position. Nevertheless, after taking serial variation into account, it is possible to compare the anterior-most preserved dorsal vertebrae of *Dreadnoughtus* to that of *Puertasaurus*. The neural arch laminae of the *Puertasaurus* dorsal vertebra are significantly more robust than those of the anterior-most preserved (fourth?) dorsal vertebra of *Dreadnoughtus.* The striking difference in the thicknesses of these laminae is unlikely to be due solely to the differing serial positions and sizes of these vertebrae. Furthermore, in *Puertasaurus*, the transverse processes of the preserved dorsal vertebra are oriented perpendicular to the sagittal plane, whereas in *Dreadnoughtus*, the transverse processes of the anterior-most preserved dorsal vertebra are oriented anterolaterally (see Supplementary Fig. 11 in dorsal view), a condition that Novas et al.[22] associated with derived titanosaurs. Additionally, the transverse processes of the *Puertasaurus* dorsal vertebra are markedly dorsoventrally deep; in *Dreadnoughtus*, by contrast, the dorsal vertebral transverse processes are shallow, as in *Futalognkosaurus*[23].

In sum, the lack of lateral expansion of the neural spine, the coalescence of the spinoprezygapophyseal laminae and the resulting dorsal closure of the spinoprezygapophyseal fossa, and the pronounced spinoprezygapophyseal lamina on the dorsal surface of the prezygapophysis all distinguish the posterior cervical vertebra of MPM-PV 1156 from that of MPM-10002. Additionally, within the anterior dorsal vertebral series, the relative gracility of the neural arch laminae and the dorsoventral shallowness and anterolateral orientation of the transverse processes differentiate material pertaining to the new taxon from MPM-10002. These differences support the taxonomic distinction of *Dreadnoughtus schrani* from *Puertasaurus reuili*.

6. Humeral histology of *Dreadnoughtus*

The bone tissue of the humerus of the *Dreadnoughtus* holotype (MPM-PV 1156) has been extensively remodelled throughout the inner cortex, being comprised of densely packed (though not completely overlapping) secondary osteons. This heavy remodelling abruptly terminates approximately 2.5 mm from the periosteal surface in a nearly linear remodelling front (Fig. 2G, arrow). Between this dense area of secondary osteons and the periosteal surface, the outer cortex consists of primary fibrolamellar bone (FLB) with few, scattered secondary osteons. The fibrolamellar complex of the unremodeled primary tissue contains a large amount of woven

bone, which shows evidence of having been rapidly deposited[54-58]. The FLB tissue is well-vascularized with longitudinal vascular canals and relatively short circular canals. Osteological markers for cessation of growth such as lamellar-zonal bone, annuli, lines of arrested growth (LAGs), avascular tissue, or an external fundamental system (EFS)[54,56,57,59] are not observed.

7. Additions and changes to the Carballido and Sander[1] matrix

In adding *Dreadnoughtus* to the phylogenetic data matrix recently published by Carballido and Sander[1], we encountered three characters that necessitated scoring changes from those presented by these authors.

(1) Character 237: Mannion and Otero[60] stated that *Mendozasaurus* and *Alamosaurus* possess one and two ventrolateral processes, respectively, on the proximal scapula. This is confirmed by images in the literature[60,61]. Accordingly, for this character, we changed the scores for these two taxa to state 1 (present).

(2) Character 268: As presented by Carballido and Sander[1], the states for this character are "3 or more (0); 2 or fewer (1)." *Alamosaurus* and *Opisthocoelicaudia* were both originally scored as inapplicable ('-') here. Neither of these titanosaurs possesses ossified carpal elements; however, the possession of zero carpals is included in Carballido and Sander's[1] state 1, so we altered the scores for these taxa accordingly.

(3) Character 306: Carballido and Sander[1] scored *Epachthosaurus* and *Rapetosaurus* as having state 1, distal femoral condyles "beveled dorsomedially approximately 10° relative to femoral shaft." However, these taxa were originally coded as lacking this feature (i.e., state 0) by Wilson[62] and Carballido et al.[63]. Published photographs demonstrate that the femoral condyles of these titanosaurs are not beveled dorsomedially. Accordingly, for this character, we changed the scores for *Epachthosaurus* and *Rapetosaurus* to state 0: distal femoral condyles "perpendicular or slightly beveled dorsolaterally."

Incorporation of these changes yields the same number of most parsimonious trees and the same strict consensus topology that was presented by Carballido and Sander[1].

Additionally, to more thoroughly investigate the interrelationships of giant titanosaurians, we added *Futalognkosaurus dukei* to Carballido and Sander's[1] matrix. Our scores for *Futalognkosaurus* for the 341 morphological characters employed by these authors were based on the description provided by Calvo et al.[24], and are as follows:

?????????? ?????????? ?????????? ?????????? ?????????? ?????????? ?????????? ?????????? ?????????? ?????????? ????????20 1??0-?0002 ?00?10?0?1 10-310002? ?121-11??2 120??0???? ?101?01??- ???2?1???? 3??010?0?1 0????????? ?????????? ?????????? ????????1? ?????????? ?????????? ?????????? ?????????? ?????????? ????1??000 00111100?? ?????????? ?????????? ?????????? ?????????? ?

8. Supplementary figures 1 to 20

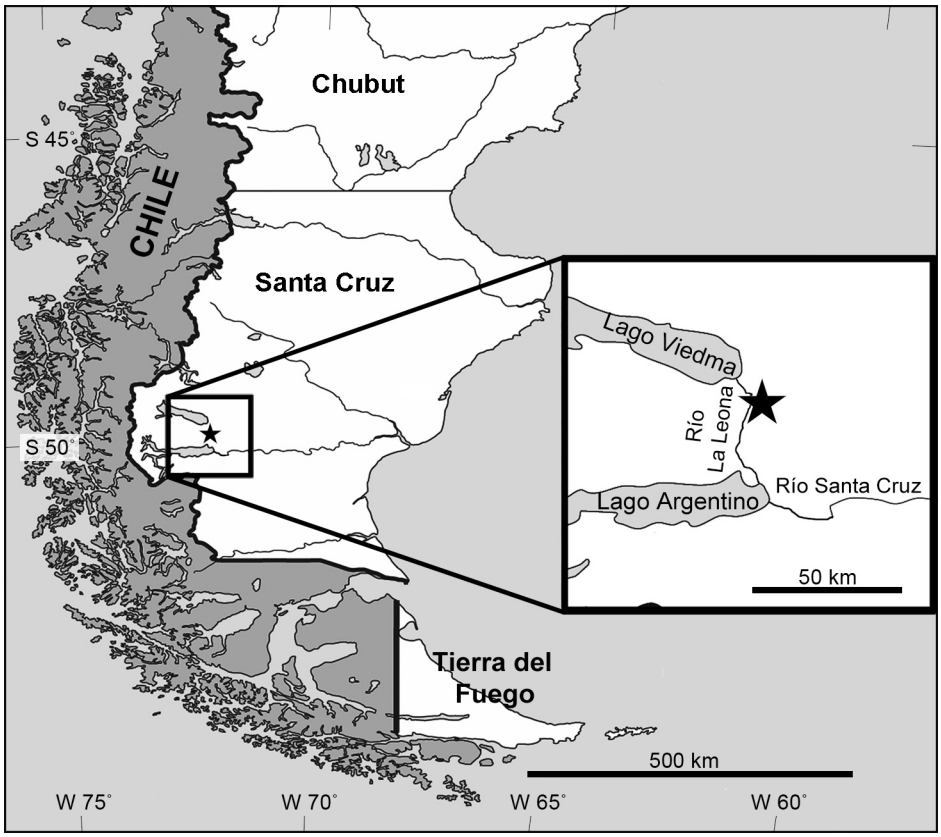

Supplementary Fig. 1. Type locality of *Dreadnoughtus schrani* (indicated by star) in south-western Santa Cruz Province, southern Patagonia, Argentina. (Base map modified from "Mapa de la provincia de Santa Cruz" by Mikelzubi, licensed under CC BY-SA 3.0.)

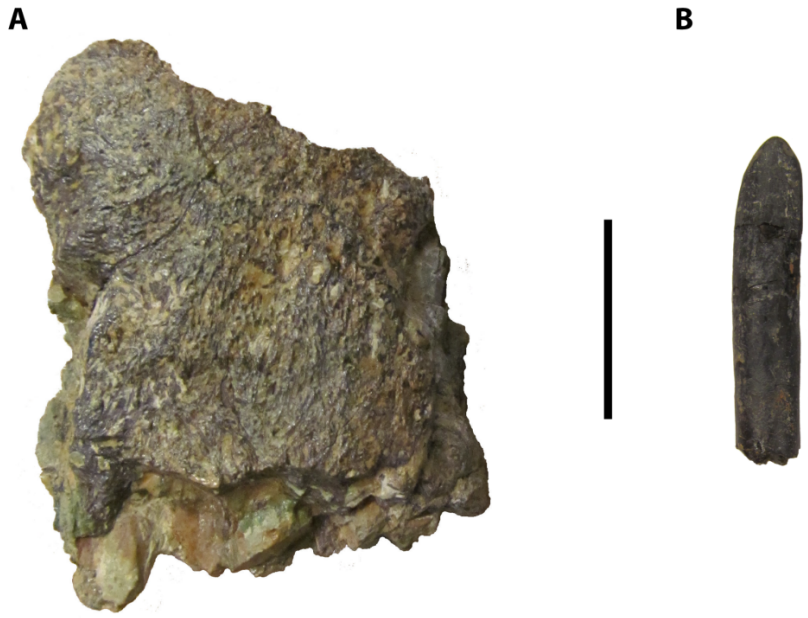

Supplementary Fig. 2. Craniodental remains of *Dreadnoughtus schrani* (MPM-PV 1156). (**A**) Maxilla fragment in lateral view. (**B**) Tooth in labial view. Scale bar equals 2 cm.

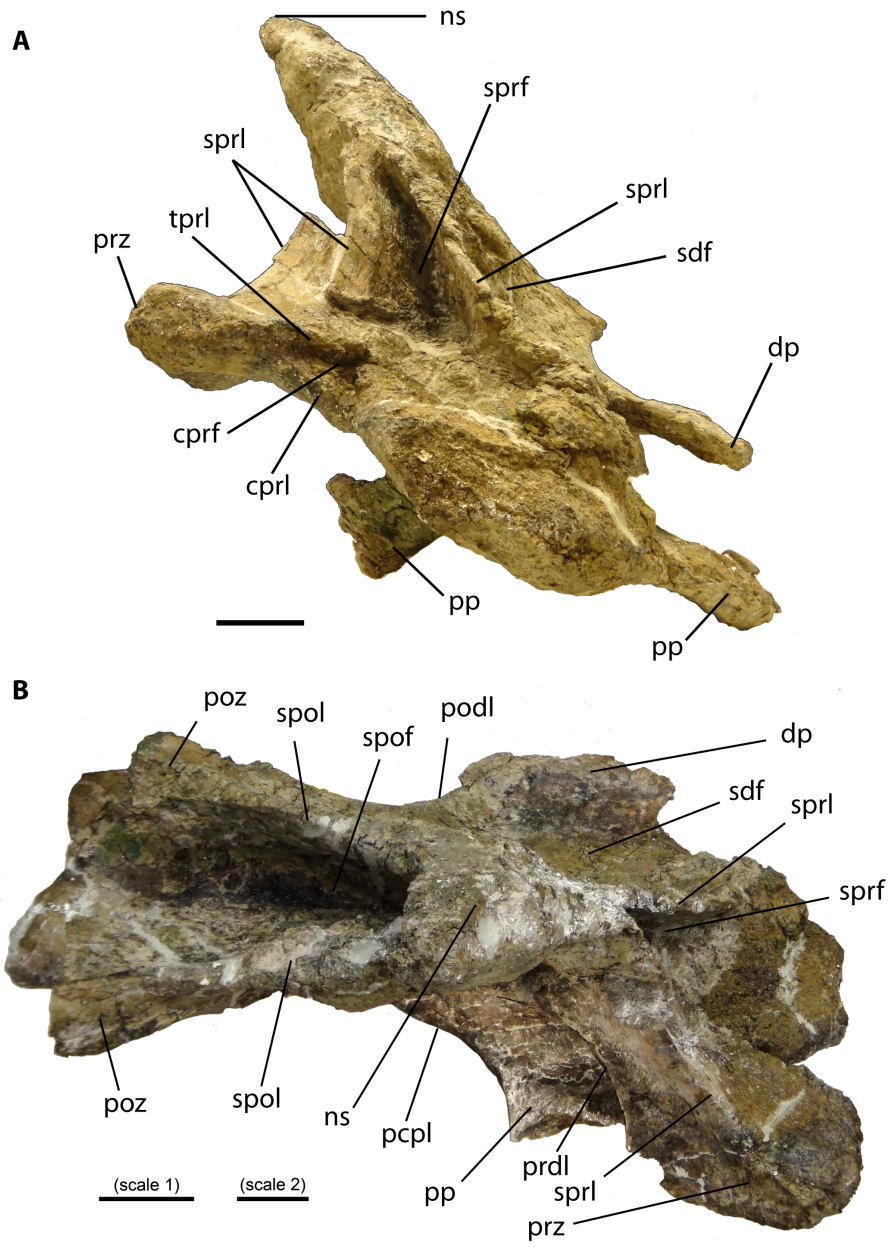

Supplementary Fig. 3. Posterior (~9th) cervical vertebra of *Dreadnoughtus schrani* (MPM-PV 1156) in (**A**) anterior and (**B**) dorsal views. Abbreviations: cprf, centroprezygapophyseal fossa; cprl, centroprezygapophyseal lamina; dp, diapophysis; ns, neural spine; pcpl, posterior centroparapophyseal lamina; podl, postzygodiapophyseal lamina; poz, postzygapophysis; pp, parapophysis; prdl, prezygodiapophyseal lamina; prz, prezygapophysis; sdf, spinodiapophyseal fossa; spof, spinopostzygapophyseal fossa; spol, spinopostzygapophyseal lamina; sprf, spinoprezygapophyseal fossa; sprl, spinoprezygapophyseal lamina; tprl, intraprezygapophyseal lamina. Scale bar in A equals 10 cm. Left scale bar in B (scale 1) equals 10 cm at the dorsoventral level of the postzygapophyses. Right scale bar in B (scale 2) equals 10 cm at the level of the parapophysis.

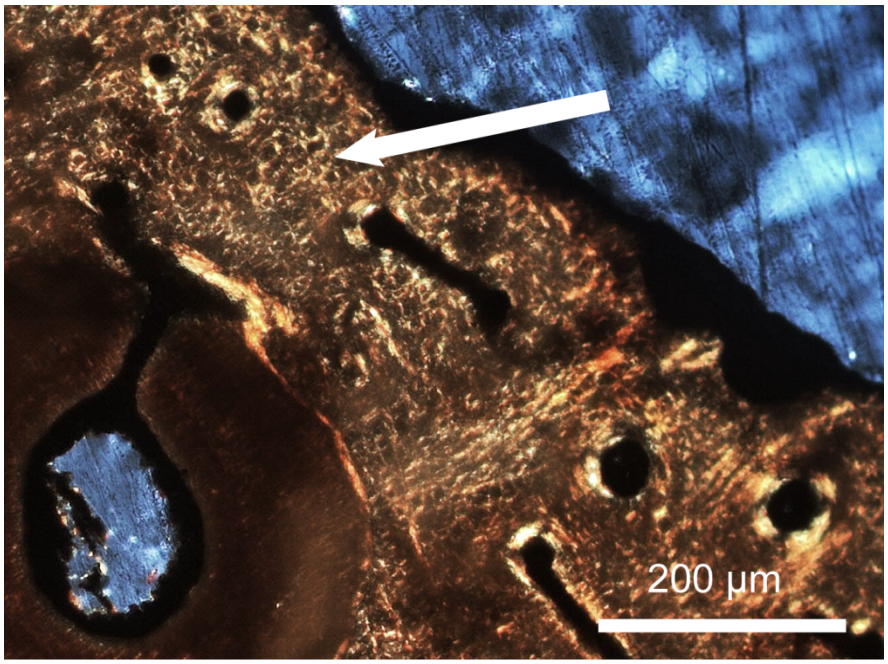

Supplementary Fig. 4. Transverse ground thin section of posterior cervical rib shaft of *Dreadnoughtus schrani* (MPM-PV 1156), imaged under cross-polarized light. Arrow indicates mineralized collagen fibril bundles, the presence of which demonstrates that this part of the cervical rib is derived from ossified tendon rather than periosteal bone.

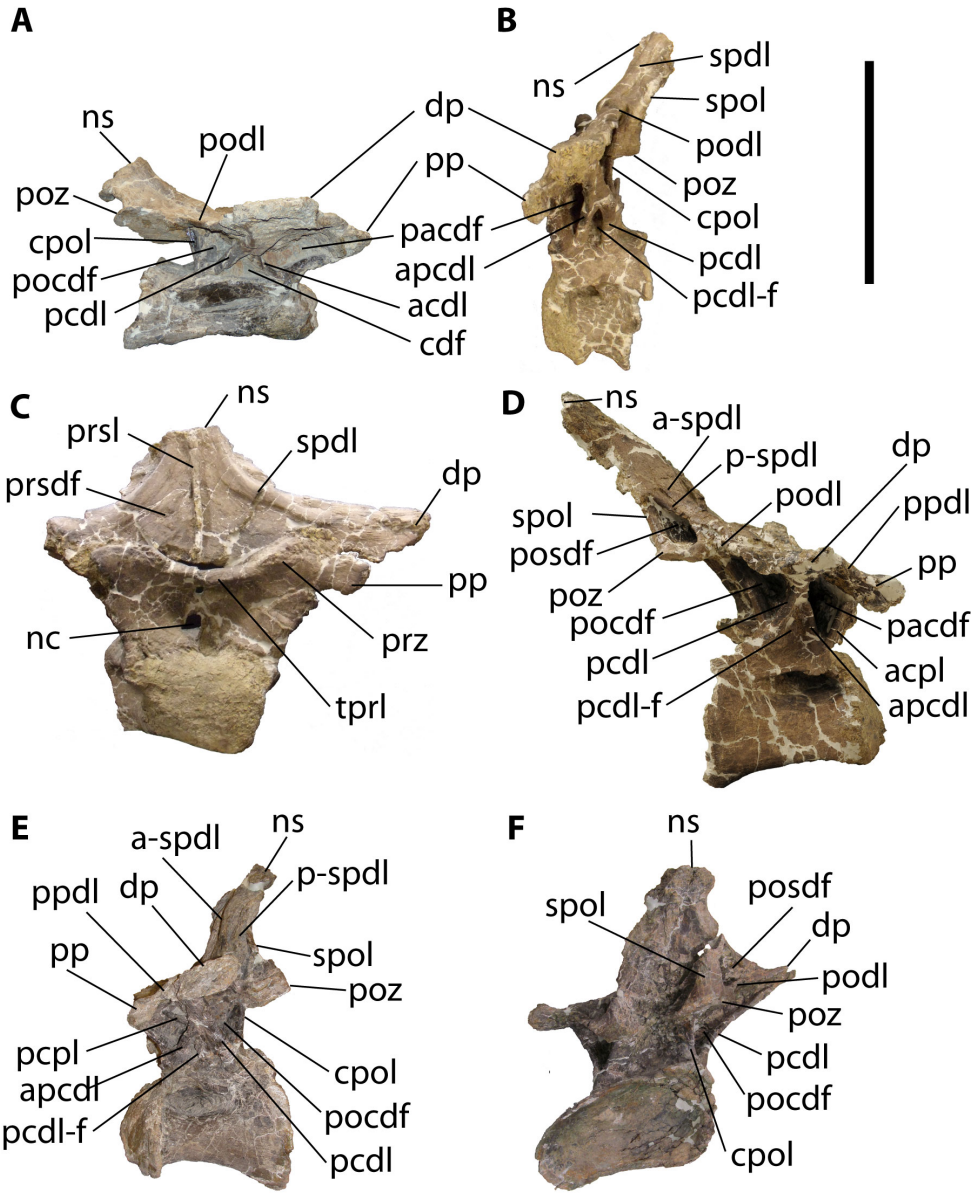

Supplementary Fig. 5. Dorsal vertebrae of *Dreadnoughtus schrani*. (**A**) Anterior (~4th) dorsal vertebra in right lateral view. Middle (~6th) dorsal vertebra in (**B**) left lateral and (**C**) anterior views. (**D**) Posterior (~7th) dorsal vertebra in right lateral view. Posterior (~8th) dorsal vertebra in (**E**) left lateral and (**F**) posterior views. Abbreviations: acpl, anterior centroparapophyseal lamina; apcdl, accessory posterior centrodiapophyseal lamina; a-spdl, anterior ramus of spinodiapophyseal lamina; cdf, centrodiapophyseal fossa; cpol, centropostzygapophyseal lamina; dp, diapophysis; nc, neural canal; ns, neural spine; pacdf, parapophyseal centrodiapophyseal fossa; pcdl, posterior centrodiapophyseal lamina; pcdl-f, posterior centrodiapophyseal fossa; pcpl, posterior centroparapophyseal lamina; pocdf, postzygapophyseal centrodiapophyseal fossa; podl, postzygodiapophyseal lamina; posdf, postzygapophyseal spinodiapophyseal fossa; poz, postzygapophysis; pp, parapophysis; ppdl, paradiapophyseal lamina; prsdf, prezygapophyseal spinodiapophyseal fossa; prsl, prespinal lamina; prz, prezygapophysis; p-spdl, posterior ramus of spinodiapophyseal lamina; spdl, spinodiapophyseal lamina; spol, spinopostzygapophyseal lamina; tprl, intraprezygapophyseal lamina. Scale bar equals 50 cm.

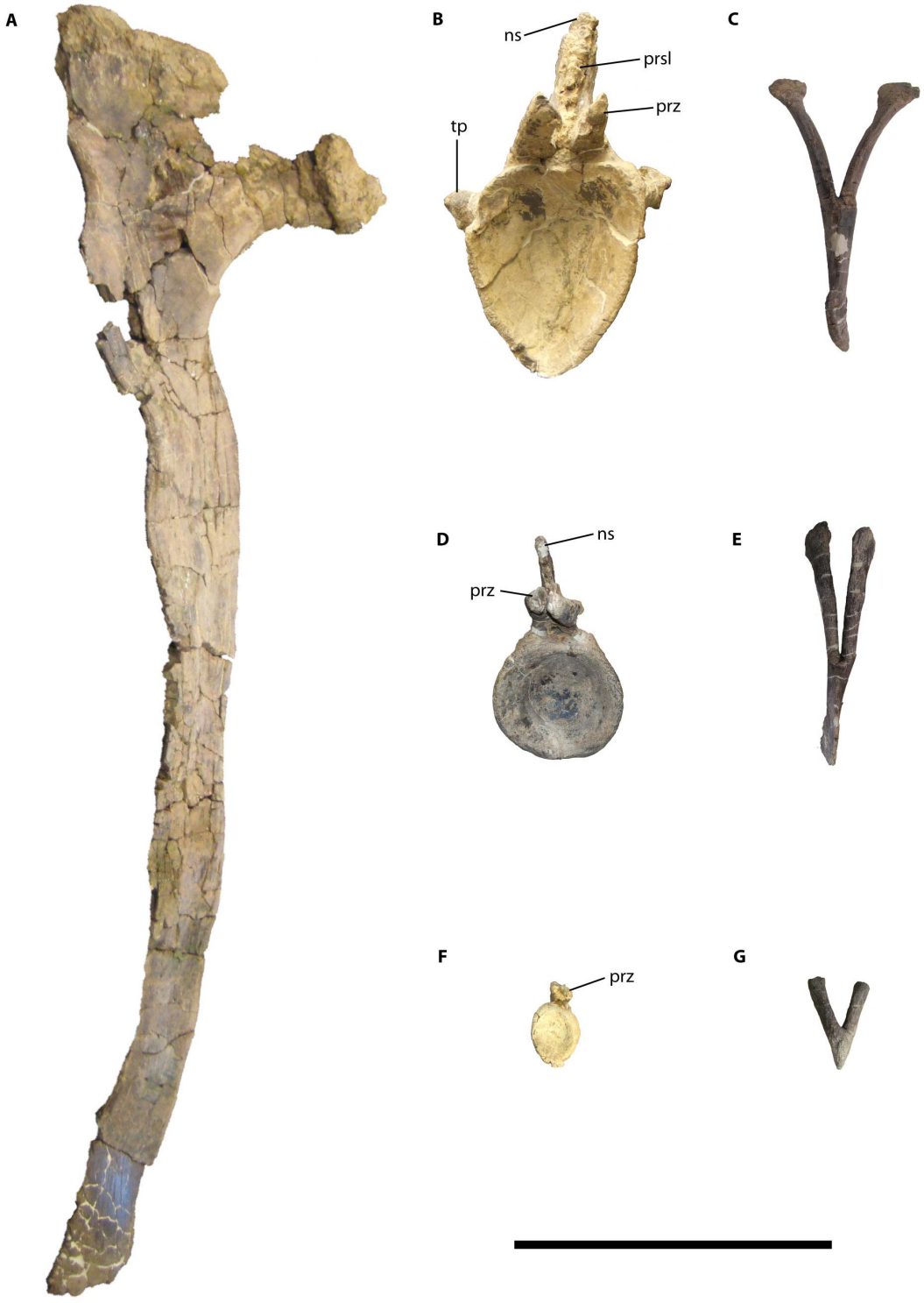

Supplementary Fig. 6. Dorsal rib and caudal skeletal anatomy of *Dreadnoughtus schrani* (MPM-PV 1156). Anterior view. (**A**) Dorsal rib. (**B**) Anterior (6^{th}) caudal vertebra. (**C**) Anterior (4^{th}) haemal arch. (**D**) Middle (15^{th}) caudal vertebra. (**E**) Middle (10^{th}) haemal arch. (**F**) Posterior caudal vertebra. (**G**) Posterior (17^{th}) haemal arch. Abbreviations: ns, neural spine; prsl, prespinal lamina; prz, prezygapophysis; tp, transverse process. Scale bar equals 50 cm.

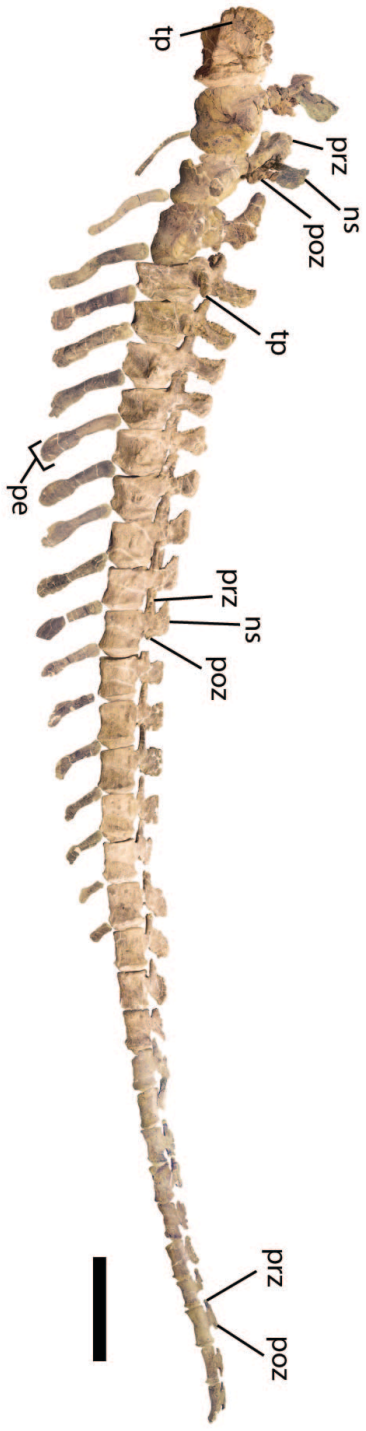

Supplementary Fig. 7. First 32 caudal vertebrae and all 18 haemal arches of *Dreadnoughtus schrani* (MPM-PV 1156) in left lateral view (positions of first 21 caudal vertebrae and haemal arches 4 to 18 are known with certainty). Abbreviations: ns, neural spine; pe, paddle-shaped distal expansion; poz, postzygapophysis; prz, prezygapophysis; tp, transverse process. Scale bar equals 1 m.

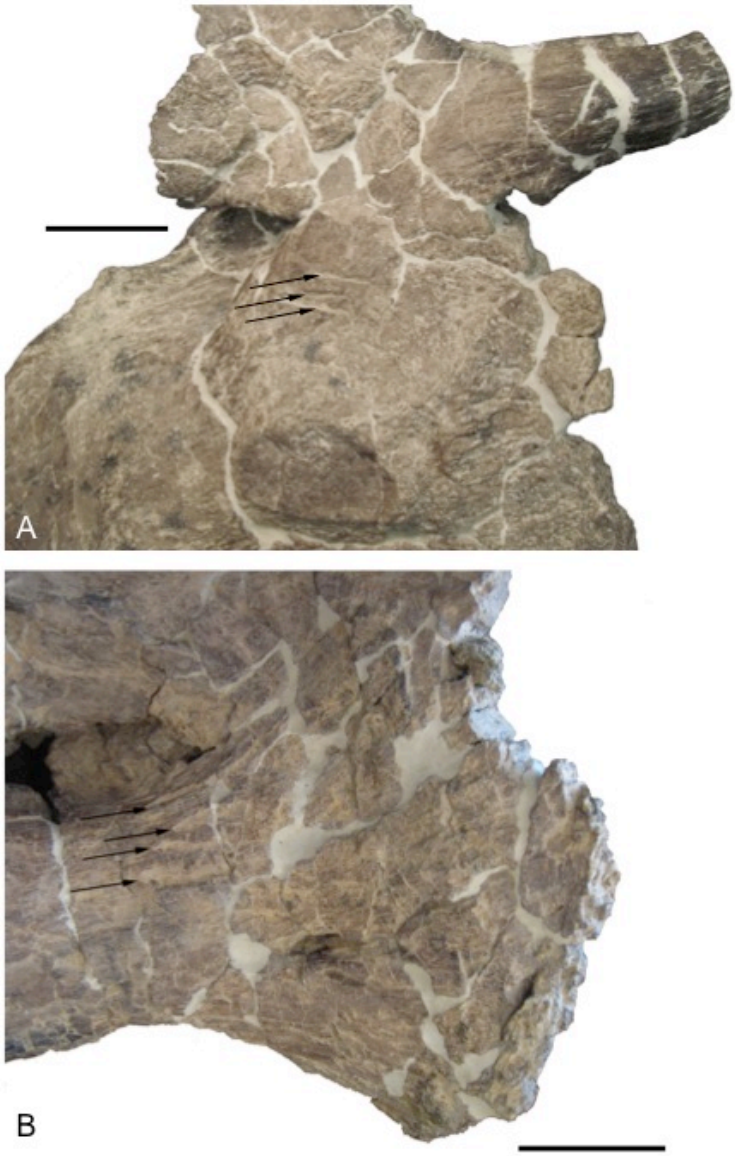

Supplementary Fig. 8. Putative scavenging marks on vertebrae of *Dreadnoughtus schrani*. (**A**) Enlargement of the right lateral face of an anterior caudal vertebra of the paratype (MPM-PV 3546), showing three potential tooth marks in the form of elongate grooves with tapering ends (indicated by arrows). (**B**) Enlargement of the left lateral face of a centrum of a middle dorsal vertebra, showing four potential tooth marks in the form of elongate depressions with tapering ends (indicated by arrows). Scale bars equal 5 cm.

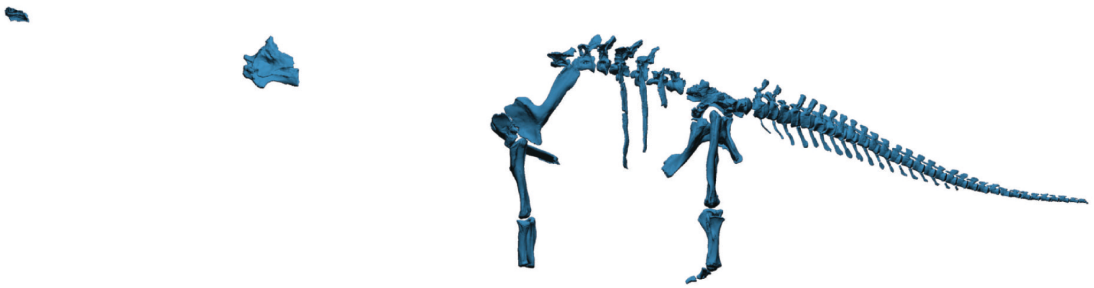

Supplementary Fig. 9. Digital reconstruction of known skeletal elements of *Dreadnoughtus schrani* (MPM-PV 1156 and MPM-PV 3546) in left lateral view. In the reconstruction, two left and one right dorsal ribs were mirrored to yield a total of six representative ribs. Moreover, except for the sternal plate, the right pectoral girdle and forelimb were mirrored from the left. The right femur, fibula, and astragalus were also mirrored from the left side, whereas the left metatarsals and pedal ungual were mirrored from the right. Downloadable, interactive 3D PDF file available here: http://dx.doi.org/10.6084/m9.figshare.1119790

[Note: all 3D PDF files, Supplementary Figures 9-18, may be downloaded here: http://dx.doi.org/10.6084/m9.figshare.1130885]

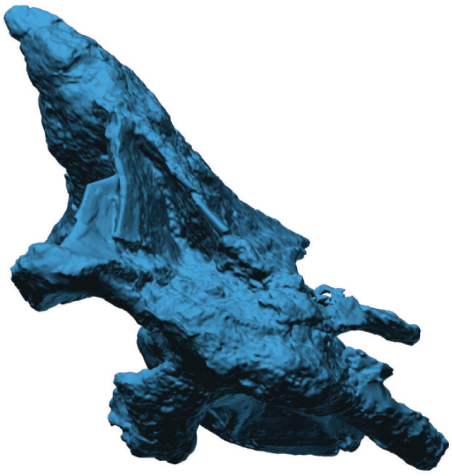

Supplementary Fig. 10. Digital image of a posterior (~9th) cervical vertebra of *Dreadnoughtus schrani* (MPM-PV 1156) in anterior view. Downloadable, interactive 3D PDF file available here: http://dx.doi.org/10.6084/m9.figshare.1119782

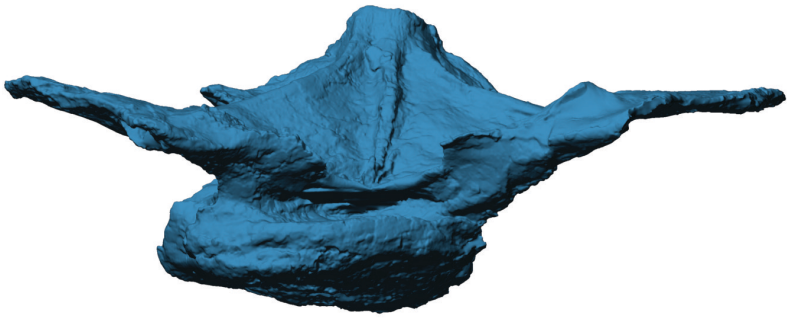

Supplementary Fig. 11. Digital image of an anterior (~4th) dorsal vertebra of *Dreadnoughtus schrani* in anterior view. Downloadable, interactive 3D PDF file available here: http://dx.doi.org/10.6084/m9.figshare.1119781

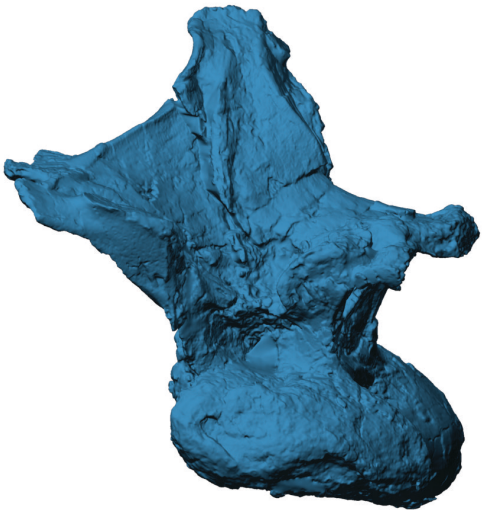

Supplementary Fig. 12. Digital image of a posterior (~8th) dorsal vertebra of *Dreadnoughtus schrani* in anterior view. Downloadable, interactive 3D PDF file available here: http://dx.doi.org/10.6084/m9.figshare.1119783

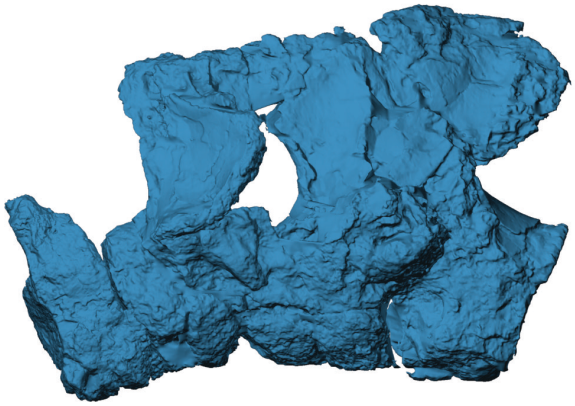

Supplementary Fig. 13. Digital image of the sacrum of *Dreadnoughtus schrani* (MPM-PV 1156) in dorsal view. Downloadable, interactive 3D PDF file available here: http://dx.doi.org/10.6084/m9.figshare.1119788

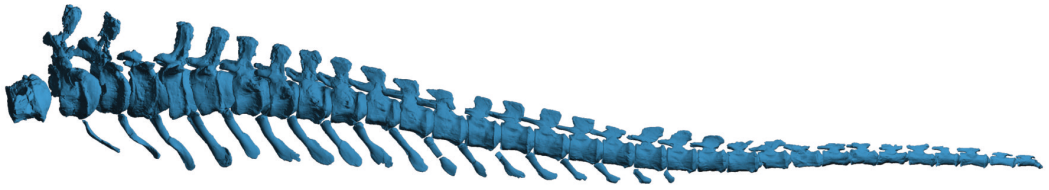

Supplementary Fig. 14. Digital reconstruction of the first 32 caudal vertebrae and associated haemal arches of the holotype of *Dreadnoughtus schrani* (MPM-PV 1156) in left lateral view. Downloadable, interactive 3D PDF file available here: http://dx.doi.org/10.6084/m9.figshare.1119785

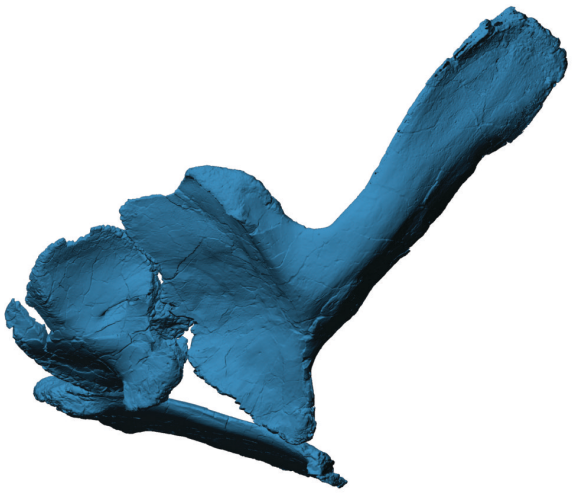

Supplementary Fig. 15. Digital reconstruction of the left shoulder girdle of *Dreadnoughtus schrani* (MPM-PV 1156) in lateral view. Downloadable, interactive 3D PDF file available here: http://dx.doi.org/10.6084/m9.figshare.1119789

Supplementary Fig. 16. Digital reconstruction of the left forelimb (minus the manus) of *Dreadnoughtus schrani* (MPM-PV 1156) in anterior view. Downloadable, interactive 3D PDF file available here: http://dx.doi.org/10.6084/m9.figshare.1119786

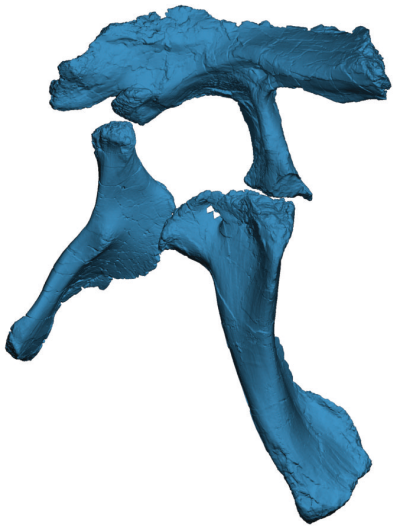

Supplementary Fig. 17. Digital reconstruction of the pelvic girdle of *Dreadnoughtus schrani* (MPM-PV 1156) in right lateral view. Downloadable, interactive 3D PDF file available here: http://dx.doi.org/10.6084/m9.figshare.1119787

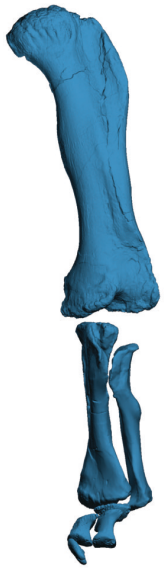

Supplementary Fig. 18. Digital reconstruction of all known skeletal elements of the hind limb of *Dreadnoughtus schrani* (MPM-PV 1156) in anterior view. Femur and fibula from left side; tibia, metatarsals, and ungual mirrored from right side. Downloadable, interactive 3D PDF file available here: http://dx.doi.org/10.6084/m9.figshare.1119784

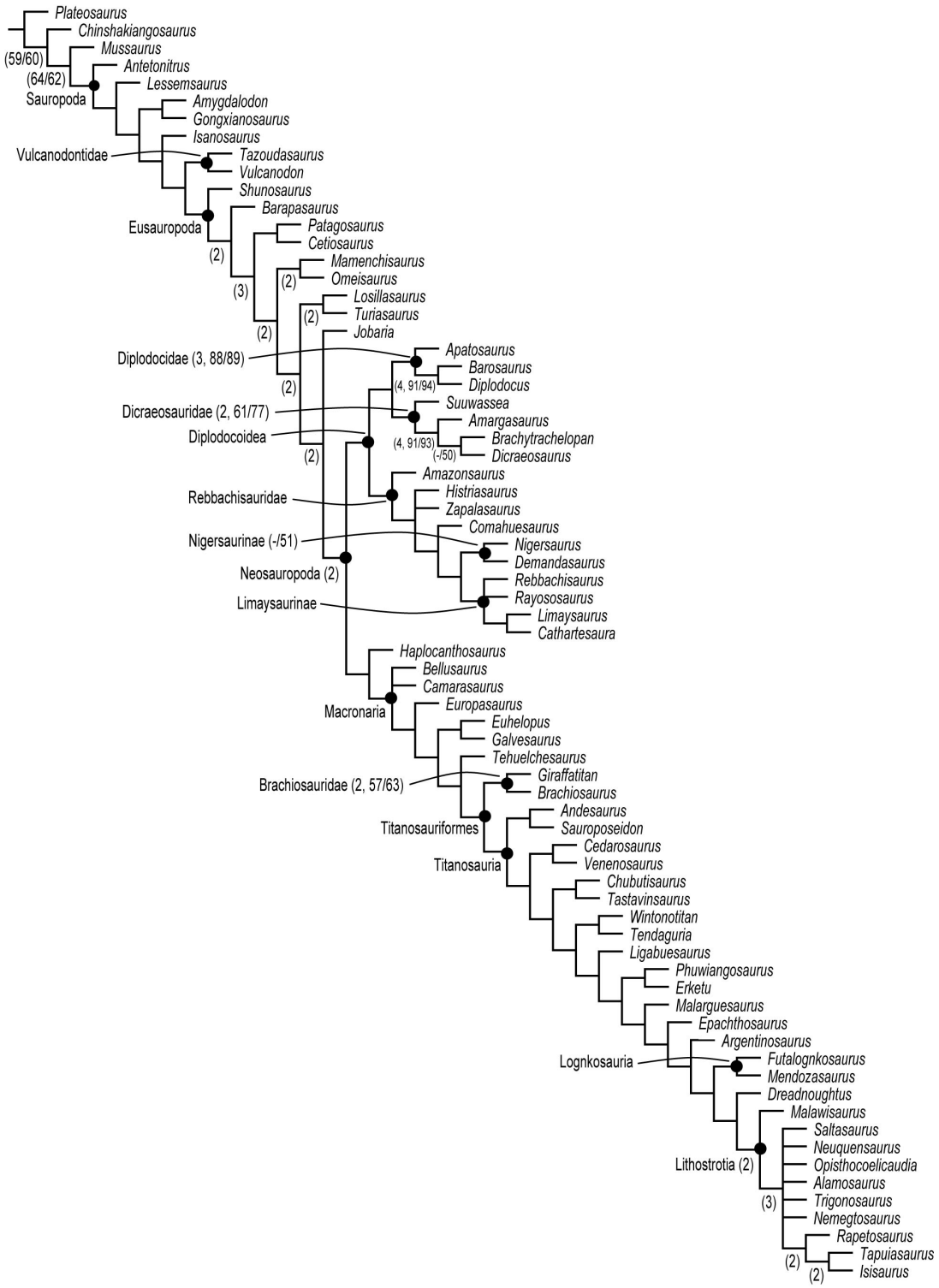

Supplementary Fig. 19. Strict consensus of ten most parsimonious trees of 1,028 steps recovered by first iteration of phylogenetic analysis that included 72 taxa (*Dreadnoughtus schrani*, *Futalognkosaurus dukei*, plus all 70 taxa analysed by Carballido and Sander[1]). Bremer indices and bootstrap and jack-knife values are presented adjacent to nodes in the following format: (Bremer index, bootstrap/jack-knife).

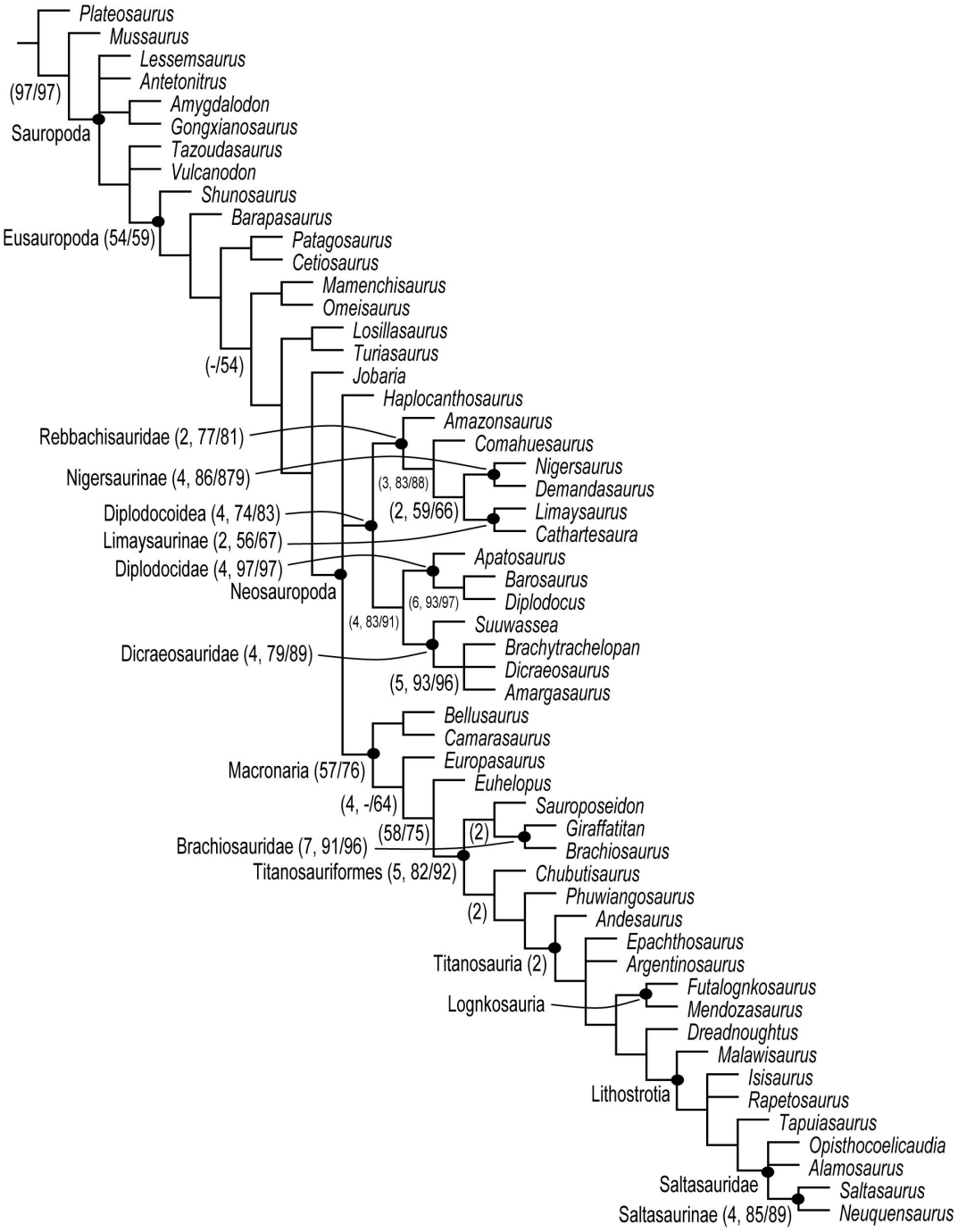

Supplementary Fig. 20. Strict consensus of 30 most parsimonious trees of 943 steps recovered by a pruned phylogenetic analysis after removal of 18 of the 20 fragmentary and unstable taxa removed in fig. 30 of Carballido and Sander[1] (we retained *Andesaurus* to define the node-based clade Titanosauria, and *Argentinosaurus* to investigate the relationship between *Dreadnoughtus* and this comparably gigantic taxon). Bremer indices and bootstrap and jack-knife values are presented adjacent to nodes in the following format: (Bremer index, bootstrap/jack-knife).

9. Supplementary tables 1 to 3

Supplementary Table 1. Measurements of holotype (MPM-PV 1156) and paratype (MPM-PV 3546) specimens of *Dreadnoughtus schrani*. The single preserved anterior cervical vertebra is listed here as part of the paratype, but this assignment should be regarded as tentative. Similarly, it is uncertain whether the anterior dorsal vertebra and two of the posterior dorsal vertebrae (the ~7th and ~8th) pertain to the holotype or paratype; here, they are tentatively assigned to the holotype. ~ = element incomplete, measurement as preserved; * = estimate generated from doubling bilateral structure preserved on only one side; L = left; R = right.

ELEMENT/DIMENSION	MPM-PV 1156	MPM-PV 3546
Dentition		
Isolated tooth		
Apicobasal length	35	
Mesiodistal length, base	7.0	
Labiolingual width, base	6.4	
Mesiodistal length, apical wear facet	4.3	
Labiolingual width, apical wear facet	2.7	
Axial Skeleton		
Cervical vertebrae		
Anterior (~4th) cervical vertebra		
Dorsoventral height, posterior centrum cotyle		~95
Transverse width, posterior centrum cotyle		~360
Posterior (~9th) cervical vertebra		
Anteroposterior length, centrum	1130	
Anteroposterior length, centrum (without anterior condyle)	930	
Dorsoventral height, anterior centrum condyle	~190	
Transverse width, anterior centrum condyle	~240	
Dorsoventral height, posterior centrum cotyle	~230	
Transverse width, posterior centrum cotyle	~370	
Dorsoventral height, maximum	850	
Dorsoventral height, neural arch	660	
Transverse width, maximum (across diapophyses)	760*	
Dorsal vertebrae		
Anterior (~4th) dorsal vertebra		
Anteroposterior length, centrum	400	
Anteroposterior length, centrum (without anterior condyle)	305	
Dorsoventral height, posterior centrum cotyle	195	
Transverse width, posterior centrum cotyle	460	

Dorsoventral height, maximum	440
Transverse width, maximum (across diapophyses)	1100

Middle (~5th) dorsal vertebra

Anteroposterior length, centrum	470
Anteroposterior length, centrum (without anterior condyle)	320
Dorsoventral height, anterior centrum condyle	470
Dorsoventral height, posterior centrum cotyle	~330
Dorsoventral height, maximum	~762

Middle (~6th) dorsal vertebra

Anteroposterior length, centrum	200
Anteroposterior length, centrum (without anterior condyle)	~180
Dorsoventral height, anterior centrum condyle	215
Transverse width, anterior centrum condyle	325
Dorsoventral height, posterior centrum cotyle	310
Transverse width, posterior centrum cotyle	415
Dorsoventral height, maximum	770
Transverse width, maximum (across diapophyses)	990*

Posterior (~7th) dorsal vertebra

Anteroposterior length, centrum	~300
Anteroposterior length, centrum (without anterior condyle)	260
Dorsoventral height, anterior centrum condyle	190
Transverse width, anterior centrum condyle	360
Dorsoventral height, posterior centrum cotyle	210
Transverse width, posterior centrum cotyle	430
Dorsoventral height, maximum	900
Transverse width, maximum (across diapophyses)	~820

Posterior (~8th) dorsal vertebra

Anteroposterior length, centrum	350
Anteroposterior length, centrum (without anterior condyle)	270
Dorsoventral height, anterior centrum condyle	170
Transverse width, anterior centrum condyle	410
Dorsoventral height, posterior centrum cotyle	240
Transverse width, posterior centrum cotyle	470
Dorsoventral height, maximum	740
Transverse width, maximum (across diapophyses)	~770

Posterior (~9th) dorsal vertebra

Anteroposterior length, centrum	410

Posterior (~10th) dorsal vertebra

Anteroposterior length, centrum	330
Anteroposterior length, centrum (without anterior condyle)	225
Dorsoventral height, posterior centrum cotyle	~310
Transverse width, posterior centrum cotyle	~335

Sacral vertebrae

Anteroposterior length along midline axis, partial sacrum	~850
Dorsoventral height, posterior face of last sacral vertebra	150
Mediolateral width, midline axis–lateral centrum rim of last sacral vertebra	200
Mediolateral width, midline axis–lateral edge of 2nd sacral rib	480
Mediolateral width, midline axis–lateral edge of 4th sacral rib	510
Mediolateral width, midline axis–lateral edge of 6th sacral rib	580

Caudal vertebrae

Caudal vertebra 1 (biconvex)

Anteroposterior length, centrum without condyles	200
Dorsoventral height, anterior centrum condyle	250
Dorsoventral height, posterior centrum condyle	310
Transverse width, anterior centrum condyle	320
Transverse width, posterior centrum condyle	310
Mediolateral length, transverse process	285
Dorsoventral height, base of transverse process	200
Estimated total width (by doubling transverse process length)	880*

Caudal vertebra 2

Anteroposterior length, centrum	350
Anteroposterior length, centrum without condyle	190
Dorsoventral height, centrum	340

Caudal vertebra 3

Anteroposterior length, centrum	300
Anteroposterior length, centrum without condyle	180
Dorsoventral height, centrum	330
Dorsoventral height, neural arch	390

Caudal vertebra 4

Anteroposterior length, centrum	330
Anteroposterior length, centrum without condyle	190
Dorsoventral height, centrum	310

(Start of articulated series)

Caudal vertebra 5

Anteroposterior length, centrum	295
Anteroposterior length, centrum without condyle	132
Dorsoventral height, centrum	332
Dorsoventral height, neural arch	311

Caudal vertebra 6

Anteroposterior length, centrum	313
Anteroposterior length, centrum without condyle	191
Dorsoventral height, centrum	272
Dorsoventral height, neural arch	279

Caudal vertebra 7

Anteroposterior length, centrum	292
Anteroposterior length, centrum without condyle	195
Dorsoventral height, centrum	135
Dorsoventral height, neural arch	241

Caudal vertebra 8

Anteroposterior length, centrum	265
Anteroposterior length, centrum without condyle	168
Dorsoventral height, centrum	136
Dorsoventral height, neural arch	204

Caudal vertebra 9

Anteroposterior length, centrum	293
Anteroposterior length, centrum without condyle	205
Dorsoventral height, centrum	261
Dorsoventral height, neural arch	204

Caudal vertebra 10

Anteroposterior length, centrum	291
Anteroposterior length, centrum without condyle	193
Dorsoventral height, centrum	222
Dorsoventral height, neural arch	198

Caudal vertebra 11

Anteroposterior length, centrum	272
Anteroposterior length, centrum without condyle	204
Dorsoventral height, centrum	251
Dorsoventral height, neural arch	171

Caudal vertebra 12

Anteroposterior length, centrum	295
Anteroposterior length, centrum without condyle	202
Dorsoventral height, centrum	211
Dorsoventral height, neural arch	146

Caudal vertebra 13

Anteroposterior length, centrum	291
Anteroposterior length, centrum without condyle	200
Dorsoventral height, centrum	201
Dorsoventral height, neural arch	122

Caudal vertebra 14

Anteroposterior length, centrum	253
Anteroposterior length, centrum without condyle	187
Dorsoventral height, centrum	202
Dorsoventral height, neural arch	131

Caudal vertebra 15

Anteroposterior length, centrum	261
Anteroposterior length, centrum without condyle	192
Dorsoventral height, centrum	183
Dorsoventral height, neural arch	125

Caudal vertebra 16

Anteroposterior length, centrum	260
Anteroposterior length, centrum without condyle	212
Dorsoventral height, centrum	178
Dorsoventral height, neural arch	122

Caudal vertebra 17

Anteroposterior length, centrum	261
Anteroposterior length, centrum without condyle	195
Dorsoventral height, centrum	180
Dorsoventral height, neural arch	115

Caudal vertebra 18

Anteroposterior length, centrum	245
Anteroposterior length, centrum without condyle	191
Dorsoventral height, centrum	172
Dorsoventral height, neural arch	85

Caudal vertebra 19

Anteroposterior length, centrum	251
Anteroposterior length, centrum without condyle	190
Dorsoventral height, centrum	165
Dorsoventral height, neural arch	123

Caudal vertebra 20

Anteroposterior length, centrum	246
Anteroposterior length, centrum without condyle	194
Dorsoventral height, centrum	157
Dorsoventral height, neural arch	115

Caudal vertebra 21

Anteroposterior length, centrum	225
Anteroposterior length, centrum without condyle	181
Dorsoventral height, centrum	152
Dorsoventral height, neural arch	102

(End of articulated series)

Caudal vertebra 22

Anteroposterior length, centrum	240
Anteroposterior length, centrum without condyle	195
Dorsoventral height, centrum	140
Dorsoventral height, neural arch	~75

Caudal vertebra 23

Anteroposterior length, centrum	240
Anteroposterior length, centrum without condyle	189
Dorsoventral height, centrum	127
Dorsoventral height, neural arch	90

Caudal vertebra 24

Anteroposterior length, centrum	235
Anteroposterior length, centrum without condyle	185
Dorsoventral height, centrum	112
Dorsoventral height, neural arch	~55

Caudal vertebra 25

Anteroposterior length, centrum	215
Anteroposterior length, centrum without condyle	172
Dorsoventral height, centrum	110
Dorsoventral height, neural arch	60

Caudal vertebra 26

Anteroposterior length, centrum	201
Anteroposterior length, centrum without condyle	175
Dorsoventral height, centrum	105
Dorsoventral height, neural arch	55

Caudal vertebra 27

Anteroposterior length, centrum	211
Anteroposterior length, centrum without condyle	180
Dorsoventral height, centrum	95
Dorsoventral height, neural arch	~50

Caudal vertebra 28

Anteroposterior length, centrum	206
Anteroposterior length, centrum without condyle	175
Dorsoventral height, centrum	95
Dorsoventral height, neural arch	45

Caudal vertebra 29

Anteroposterior length, centrum	183
Anteroposterior length, centrum without condyle	145
Dorsoventral height, centrum	95
Dorsoventral height, neural arch	40

Caudal vertebra 30

Anteroposterior length, centrum	205
Anteroposterior length, centrum without condyle	170
Dorsoventral height, centrum	95
Dorsoventral height, neural arch	50

Caudal vertebra 31

Anteroposterior length, centrum	200
Anteroposterior length, centrum without condyle	155
Dorsoventral height, centrum	60
Dorsoventral height, neural arch	25

Caudal vertebra 32

Anteroposterior length, centrum	175
Anteroposterior length, centrum without condyle	145
Dorsoventral height, centrum	60
Dorsoventral height, neural arch	~20

Haemal arch 1 (associated with caudal vertebra 2)

Dorsoventral length	35

Haemal arch 2 (associated with caudal 3)

Dorsoventral length	43
Anteroposterior width, ventral	5

Haemal arch 3 (associated with caudal 4)

Dorsoventral length	49
Anteroposterior width, ventral	7

(Start of articulated series)

Haemal arch 4 (articulated with caudal 5)

Dorsoventral length	403
Anteroposterior width, ventral	91

Haemal arch 5 (articulated with caudal 6)

Dorsoventral length	412

Haemal arch 6 (articulated with caudal 7)

Dorsoventral length	441
Anteroposterior width, ventral	126

Haemal arch 7 (articulated with caudal 8)

Dorsoventral length	435
Anteroposterior width, ventral	112

Haemal arch 8 (articulated with caudal 9)

Dorsoventral length	422
Anteroposterior width, ventral	125

Haemal arch 9 (articulated with caudal 10)

Dorsoventral length	395
Anteroposterior width, ventral	111

Haemal arch 10 (articulated with caudal 11)

Dorsoventral length	395
Anteroposterior width, ventral	82

Haemal arch 11 (articulated with caudal 12)

Dorsoventral length	255

Haemal arch 12 (articulated with caudal 13)

Dorsoventral length	~295

Haemal arch 13 (articulated with caudal 14)

Anteroposterior width, ventral	120

Haemal arch 14 (articulated with caudal 15)

Dorsoventral length	266
Anteroposterior width, ventral	99

Haemal arch 15 (articulated with caudal 16)

Dorsoventral length	~221

Haemal arch 16 (articulated with caudal 17)

Dorsoventral length	~213
Anteroposterior width, ventral	~98

Haemal arch 17 (articulated with caudal 18)

Dorsoventral length	153
Anteroposterior width, ventral	83

Haemal arch 18 (articulated with caudal 19)

Dorsoventral length	98
Anteroposterior width, ventral	50

(End of articulated series)

Appendicular Skeleton	
Scapula	
Anteroposterior length, maximum	1740L
Dorsoventral height, maximum (anterior, glenoid–tip of acromial process)	1030L
Dorsoventral height, minimum (at mid-blade)	270L
Dorsoventral height, posterior end of blade	360L
Coracoid	
Dorsoventral height, maximum	680L
Anteroposterior length, maximum	580L
Dorsoventral height, coracoid foramen–ventral border	370L
Anteroposterior length, coracoid foramen–anterior border	410L
Anteroposterior length, glenoid	350*L
Sternal plate	
Anteroposterior length, maximum	1120L, 1140R
Mediolateral width, maximum (at anterior end)	540L, 620R
Humerus	
Proximodistal length	1600L
Mediolateral width, proximal	740L
Proximodistal length, deltopectoral crest	640L
Anteroposterior thickness, minimum	120L
Mediolateral width, minimum	320L
Circumference, minimum midshaft	785L
Mediolateral width, distal	540L
Mediolateral breadth, lateral condyle	230L
Mediolateral breadth, medial condyle	280L
Mediolateral breadth, olecranon fossa	270L
Proximodistal height, olecranon fossa	110L
Radius	
Proximodistal length	950L
Mediolateral width, proximal	280L
Anteroposterior thickness, minimum	130L
Mediolateral width, minimum	140L
Mediolateral width, distal	200L

Ulna

Proximodistal length	1010L	
Mediolateral width, proximal	420L	
Anteroposterior thickness, minimum	190L	
Mediolateral width, minimum	150L	
Mediolateral width, distal	320L	

Ilium

Anteroposterior length	1310R	1240*L
Anteroposterior length, preacetabular process	640R	690L, 580R
Dorsoventral height, preacetabular process	420R	630L, 560R
Anteroposterior length, postacetabular process	220R	160*L
Dorsoventral height, postacetabular process	60R	

Pubis

Proximodistal length	1400L, 1260R	1000L, 1200R
Mediolateral width	560L, 370R	650L, 500R

Ischium

Proximodistal length	1010L, 1020R	
Mediolateral width, maximum (at distal end)	350L, 320R	

Femur

Proximodistal length	1910L	1290L
Mediolateral width, proximal	550L	670L
Mediolateral breadth, femoral head	450L	550L
Mediolateral breadth, greater trochanter	90L	190*L
Proximodistal length, femoral head–fourth trochanter	890L	610L
Mediolateral width, lateral face–fourth trochanter	330L	330L
Anteroposterior thickness, minimum	160L	180L
Mediolateral width, minimum	350L	310L
Circumference, minimum midshaft	910L	874L
Mediolateral width, distal	630L	670L
Proximodistal height, crural extensor fossa	280L	170L
Mediolateral breadth, crural extensor fossa	260L	180L
Mediolateral breadth, lateral condyle	130L	200L
Mediolateral breadth, medial condyle	140L	190L

Tibia

Proximodistal length	1090L, 1200R	
Mediolateral breadth, proximal	380L, 490R	

Proximodistal height, cnemial crest	240L, 220R
Mediolateral breadth, cnemial crest	120L, 270R
Anteroposterior thickness, minimum	200L, 200R
Mediolateral width, minimum	150L, 130R
Mediolateral breadth, distal	410L, 390R

Fibula

Proximodistal length	1030L
Mediolateral breadth, proximal	370L
Proximodistal length, proximal end–iliofibularis tubercle	340L
Anteroposterior thickness, minimum	130L
Mediolateral width, minimum	120L
Mediolateral breadth, distal	170L

Astragalus

Mediolateral width, maximum	230L
Proximodistal height, maximum (ascending process–distal condyle)	120L
Mediolateral width, distal condyle	190L

Metatarsal I

Proximodistal length	210R
Mediolateral breadth, proximal	160R
Dorsoplantar thickness, minimum	110R
Mediolateral width, minimum	130R
Mediolateral breadth, distal	160R
Mediolateral breadth, lateral condyle	70R
Mediolateral breadth, medial condyle	60R

Metatarsal II

Proximodistal length	250R
Mediolateral breadth, proximal	140R
Dorsoplantar thickness, minimum	110R
Mediolateral width, minimum	80R
Mediolateral breadth, distal	150R
Mediolateral breadth, lateral condyle	60R
Mediolateral breadth, medial condyle	60R

Pedal ungual I

Proximodistal length	230R

Supplementary Table 2. Skeletal completeness of *Dreadnoughtus schrani* versus other gigantic titanosaurian taxa.

	In a complete skeleton	*Dreadnoughtus schrani*	*Futalognkosaurus dukei*	*Paralititan stromeri*	*Argentinosaurus huinculensis*	'*Antarctosaurus*' *giganteus*	*Puertasaurus reuili*
Appendicular	64[a]	21	4	12	1	4	0
Axial	132[b]	94	35	8	12	2	4
Cranial	60[c]	1	0	0	0	0	0
Skeleton total	256	116	39	20	13	6	4
Total completeness %	100.0%	45.3%	15.2%	7.8%	5.1%	2.3%	1.6%
Postcranial total	196	115	39	20	13	6	4
Postcranial completeness %	100.0%	58.7%	19.9%	10.2%	6.6%	3.1%	2.0%
Mirrored postcranial total	142	100	38	18	13	5	4
Mirrored postcranial completeness %	100.0%	70.4%	26.8%	12.7%	9.2%	3.5%	2.8%
By body region total	31[d]	27	12	13	5	4	3
By body region completeness %	100.0%	87.1%	38.7%	41.9%	16.1%	12.9%	9.7%

[a]Counts of appendicular elements in a single individual: astragalus-2, coracoid-2, femur-2, fibula-2, humerus-2, ilium-2, ischium-2, metacarpal-10, metatarsal-10, pedal non-ungual phalanx-12, pedal ungual-6, pubis-2, radius-2, scapula-2, sternal plate-2, tibia-2, ulna-2.

[b]Counts of axial elements in a single individual: caudal vertebra-40, cervical vertebra-14, cervical rib-24, dorsal vertebra-10, dorsal rib-20, haemal arch-18, sacral vertebra and fused sacral ribs-6.

[c]Counts of cranial elements in a single individual: angular-2, articular-2, basioccipital-1, basisphenoid-1, coronoid-2, dentary-2, ectopterygoid-2, exoccipital-2, frontal-2, hyoid-2, jugal-2, lacrimal-2, laterosphenoid-2, maxilla-2, nasal-2, orbitosphenoid-2, palatine-2, parasphenoid-1, parietal-2, postorbital-2, prearticular-2, prefrontal-2, premaxilla-2, prootic-2, pterygoid-2, quadrate-2, quadratojugal-2, splenial-2, squamosal-2, supraoccipital-1, surangular-2, vomer-2.

[d]Regions defined as follows: cranial-1, anterior cervical-1, middle cervical-1, posterior cervical-1, cervical rib-1, anterior dorsal-1, middle dorsal-1, posterior dorsal-1, dorsal rib-1, sacral and sacral ribs-1, anterior caudal-1, middle caudal-1, posterior caudal-1, haemal arch-1, scapula-1, coracoid-1, sternal-1, humerus-1, radius-1, ulna-1, metacarpal-1, ilium-1, pubis-1, ischium-1, femur-1, tibia-1, fibula-1, astragalus-1, metatarsal-1, pedal non-ungual phalanx-1, pedal ungual-1.

Supplementary Table 3. Morphological character completeness of *Dreadnoughtus schrani* versus other titanosaurian taxa, based on the character matrix of Carballido and Sander[1]. *Dreadnoughtus* is among the best represented titanosaurs, and is dramatically more informative than the other gigantic titanosaurs *Futalognkosaurus* and *Argentinosaurus*.

Titanosaurian Taxon	Character Data (%)	Titanosaurian Taxon	Postcranial Character Data (%)
Rapetosaurus	61.0	*Opisthocoelicaudia*	85.8
Opisthocoelicaudia	58.7	***Dreadnoughtus***	**81.1**
Saltasaurus	57.8	*Saltasaurus*	76.0
Dreadnoughtus	**57.5**	*Alamosaurus*	74.7
Alamosaurus	53.4	*Neuquensaurus*	70.8
Neuquensaurus	48.4	*Isisaurus*	62.2
Malawisaurus	45.5	*Malawisaurus*	58.4
Isisaurus	42.5	*Rapetosaurus*	56.2
Tapuiasaurus	39.9	*Epachthosaurus*	51.5
Epachthosaurus	35.2	*Mendozasaurus*	40.3
Mendozasaurus	27.6	*Andesaurus*	31.8
Nemegtosaurus	25.5	*Futalognkosaurus*	27.0
Andesaurus	21.7	*Tapuiasaurus*	27.0
Futalognkosaurus	18.5	*Trigonosaurus*	26.2
Trigonosaurus	17.9	*Argentinosaurus*	18.5
Argentinosaurus	12.6	*Nemegtosaurus*	0.90

10. References for Supplementary Information

1 Carballido, J. L. & Sander, P. M. Postcranial axial skeleton of *Europasaurus holgeri* (Dinosauria, Sauropoda) from the Upper Jurassic of Germany: implications for sauropod ontogeny and phylogenetic relationships of basal Macronaria. *J. Syst. Palaeontol.* **12**, 335–387 (2014).

2 Arbe, H. A. & Hechem, J. J. Estratigraphía y facies de depósitos continentales, litorales, y marinos del Cretácico superior; lago Argentino. *Actas IX Congr. Geol. Argent.* **7**, 124–158 (1984).

3 Macellari, C. E., Barrio, C. A. & Manassero, M. J. Upper Cretaceous to Paleocene depositional sequences and sandstone petrography of southwestern Patagonia (Argentina and Chile). *J. South. Am. Earth Sci.* **2**, 223–239 (1989).

4 Kraemer, P. E. & Riccardi, A. C. Estratigrafía de la región comprendida entre los lagos Argentino y Viedma (49° 40'–50° 10' lat. S), Provincia de Santa Cruz. *Rev. Asoc. Geol. Argent.* **52**, 333–360 (1997).

5 Arbe, H. A. in *Geología y Recursos Naturales de Santa Cruz: Relatorio del XV Congreso Geológica Argentino.* (Haller, M.J.) 103–128.

6 Egerton, V. M. *The Geology, Paleontology and Paleoecology of the Cerro Fortaleza Formation, Patagonia (Argentina)*. Ph.D. thesis, Drexel University (2011).

7 Feruglio, E. Relaciones estratigráficas entre el Patagoniano y el Santacruciano en la Patagonia Austral. *Rev*. *Mus*. *La Plata Sec*. *Geol*. **4**, 128–159 (1938).

8 Feruglio, E. Estudios geológicos y glaciológicos en la región del lago Argentino (Patagonia). *Bol. Acad. Nac. Cienc.* **37**, 3–255 (1944).

9 Riccardi, A. C. & Rolleri, E. O. in *II Simposio Geología Regional Argentina.* 1173–1306 (Academia Nacional de Ciencias, Córdoba).

10 Varela, A. N., Veiga, G. D. & Poiré, D. G. Sequence stratigraphic analysis of Cenomanian greenhouse palaeosols: a case study from southern Patagonia, Argentina. *Sediment. Geol.* **271–272**, 67–82 (2012).

11 Egerton, V. M., Novas, F. E., Dodson, P. & Lacovara, K. The first record of a neonatal ornithopod dinosaur from Gondwana. *Gondwana Res.* **23**, 268–271 (2013).

12 Rogers, R. R. & Kidwell, S. M. in *Bonebeds: Genesis, Analysis, and Paleobiological Significance* (Rogers, R.R., Eberth, D.A., & Fiorillo, A.R.) 1–63 (University of Chicago Press, 2007).

13 Behrensmeyer, A. K., Willis, B. J. & Quade, J. Floodplains and paleosols of Pakistan Neogene and Wyoming Paleogene deposits; a comparative study. *Palaeogeogr., Palaeocl., Palaeoecol.* **115**, 37–60 (1995).

14 Cook, E. Taphonomy of two non-marine Lower Cretaceous bone accumulations from southeastern England. *Palaeogeogr., Palaeocl., Palaeoecol.* **116**, 263–270 (1995).

15 Willis, B. J. & Behrensmeyer, A. K. Fluvial systems in the Siwalik Miocene and Wyoming Paleogene in long records of continental ecosystems. *Palaeogeogr., Palaeocl., Palaeoecol.* **115**, 13–35 (1995).

16 González Riga, B. J. & Astini, R. A. Preservation of large titanosaur sauropods in overbank fluvial facies: a case study in the Cretaceous of Argentina. *J. S. Am. Earth Sci.* **23**, 290–303 (2007).

17 Novas, F. E., Ezcurra, M. D. & Lecuona, A. *Orkoraptor burkei* nov. gen. et sp., a large theropod from the Maastrichtian Pari Aike Formation, southern Patagonia, Argentina. *Cretac. Res.* **29**, 468–480 (2008).

18 Britt, B. B. *Pneumatic Postcranial Bones in Dinosaurs and Other Archosaurs*. Ph.D. thesis, University of Calgary (1993).

19 Britt, B. B. in *Encyclopedia of Dinosaurs*. (Currie, P. J. & Padian, K.) 590–593 (Academic Press, 1997).

20 Wedel, M. J. Vertebral pneumaticity, air sacs, and the physiology of sauropod dinosaurs. *Paleobiology* **29**, 243–255 (2003).

21 Wedel, M. J. The evolution of vertebral pneumaticity in sauropod dinosaurs. *J. Vertebr. Paleontol.* **23**, 344–357 (2003).

22 González Riga, B. J. Nuevos restos fósiles de *Mendozasaurus neguyelap* (Sauropoda, Titanosauria) del Cretácico tardío de Mendoza, Argentina. *Ameghiniana* **42**, 535–548 (2005).

23 Novas, F. E., Salgado, L., Calvo, J. & Agnolin, F. Giant titanosaur (Dinosauria, Sauropoda) from the Late Cretaceous of Patagonia. *Rev. Mus. Argent. Cienc. Nat. Nueva Ser.* **7**, 37–41 (2005).

24 Calvo, J. O., Porfiri, J. D., González Riga, B. J. & Kellner, A. W. A. Anatomy of *Futalognkosaurus dukei* Calvo, Porfiri, González Riga & Kellner, 2007 (Dinosauria, Titanosauridae) from the Neuquén Group (Late Cretaceous), Patagonia, Argentina. *Arq. Mus. Nac., Rio de Janeiro* **65**, 511–526 (2007).

25 Upchurch, P., Barrett, P. M. & Dodson, P. in *The Dinosauria, Second Edition* (Weishampel, D. B., Dodson, P., & Osmólska, H.) 259–322 (University of California Press, 2004).

26 Upchurch, P. The phylogenetic relationships of sauropod dinosaurs. *Zool. J. Linn. Soc.* **124**, 43–103 (1998).

27 Cerda, I. A. Consideraciones sobre la histogénesis de las costillas cervicales en los dinosaurios saurópodos. *Ameghiniana* **46**, 193–198 (2009).

28 Klein, N., Christian, A. & Sander, P. M. Histology shows that elongated neck ribs in sauropod dinosaurs are ossified tendons. *Biol. Lett.* **8**, 1032–1035 (2012).

29 Salgado, L., Coria, R. A. & Calvo, J. O. Evolution of titanosaurid sauropods. I: phylogenetic analysis based on the postcranial evidence. *Ameghiniana* **34**, 3–32 (1997).

30 D'Emic, M. D. & Wilson, J. A. New remains attributable to the holotype of the sauropod dinosaur *Neuquensaurus australis*, with implications for saltasaurine systematics. *Acta Palaeontol. Pol.* **56**, 61–73 (2011).

31 Martinelli, A. G. & Forasiepi, A. Late Cretaceous vertebrates from Bajo de Santa Rosa (Allen Formation), Río Negro Province, Argentina, with the description of a new

sauropod dinosaur (Titanosauridae). *Rev. Mus. Argent. Cienc. Nat. Nueva Ser.* **6**, 257–305 (2004).

32 Martínez, R. D., Giménez, O., Rodríguez, J., Luna, M. & Lamanna, M. C. An articulated specimen of the basal titanosaurian (Dinosauria: Sauropoda) *Epachthosaurus sciuttoi* from the early Late Cretaceous Bajo Barreal Formation of Chubut Province, Argentina. *J. Vertebr. Paleontol.* **24**, 107–120 (2004).

33 Powell, J. E. in *Los Dinosaurios y Su Entorno Biotico*. Actas del Segundo Curso de Paleontología en Cuenca (Sanz, J. L. & Buscalioni, A. D.) 165–230 (Institutio 'Juan de Valdes', 1992).

34 Powell, J. E. Revision of South American titanosaurid dinosaurs: palaeobiological, palaeobiogeographical and phylogenetic aspects. *Rec. Queen. Vic. Mus.* **111**, 1–173 (2003).

35 Campos, D. de A., Kellner, A. W. A., Bertini, R. J. & Santucci, R. M. On a titanosaurid (Dinosauria, Sauropoda) vertebral column from the Bauru Group, Late Cretaceous of Brazil. *Arq. Mus. Nac., Rio de Janeiro* **63**, 565–593 (2005).

36 Santucci, R. M. & Bertini, R. J. A new titanosaur from western São Paulo state, Upper Cretaceous Bauru Group, south-east Brazil. *Palaeontology* **49**, 59–66 (2006).

37 Wilson, J. A. Sauropod dinosaur phylogeny: critique and cladistic analysis. *Zool. J. Linn. Soc.* **136**, 217–276 (2002).

38 González Riga, B. J. A new titanosaur (Dinosauria, Sauropoda) from the Upper Cretaceous of Mendoza Province, Argentina. *Ameghiniana* **40**, 155–172 (2003).

39 Wilson, J. A., D'Emic, M. D., Ikejiri, T., Moacdieh, E. M. & Whitlock, J. A. A nomenclature for vertebral fossae in sauropods and other saurischian dinosaurs. *PLoS ONE* **6**, e17114 (2011).

40 Santucci, R. M. & Campos, D. de A. A new sauropod (Macronaria, Titanosauria) from the Adamantina Formation, Bauru Group, Upper Cretaceous of Brazil and the phylogenetic relationships of Aeolosaurini. *Zootaxa* **3085**, 1–33 (2011).

41 Curry Rogers, K. The postcranial osteology of *Rapetosaurus krausei* (Sauropoda: Titanosauria) from the Late Cretaceous of Madagascar. *J. Vertebr. Paleontol.* **29**, 1046–1086 (2009).

42 Martin, V. Baby sauropods from the Sao Khua Formation (Lower Cretaceous) in northeastern Thailand. *Gaia* **10**, 147–153 (1994).

43 Wilhite, R. in *Thunder-Lizards: The Sauropodomorph Dinosaurs* (Tidwell, V. & Carpenter, K.) 268–301 (Indiana University Press, 2005).

44 Kellner, A. W. A. & de Azevedo, S. A. K. in *Proceedings of the Second Gondwanan Dinosaur Symposium* (Tomida, Y., Rich, T. H. & Vickers-Rich, P.) 111–142 (National Science Museum of Tokyo, 1999).

45 Smith, J. B. *et al.* A giant sauropod dinosaur from an upper Cretaceous mangrove deposit in Egypt. *Science* **292**, 1704–1706 (2001).

46 Gomani, E. M. Sauropod dinosaurs from the Early Cretaceous of Malawi, Africa. *Palaeontol*. *Electron.* **8**, 1–37 (2005).

47 Garcia, R. A. & Salgado, L. The titanosaur sauropods from the Allen Formation (late Campanian–early Maastrichtian) of Salitral Moreno (Patagonia, Río Negro, Argentina). *Acta Palaeontol*. *Pol*. 5**8**, 269–284 (2011).

48 Filippi, L. S. & Garrido, A. C. *Pitekunsaurus macayai* gen. *et* sp. nov., nuevo titanosaurio (Saurischia, Sauropoda) del Cretácico Superior de la Cuenca Neuquina, Argentina. *Ameghiniana* **45**, 575–590 (2008).

49 Wilson, J. A. & Sereno, P. C. Early evolution and higher-level phylogeny of sauropod dinosaurs. *J*. *Vertebr*. *Paleontol*. **18**, 1–71 (1998).

50 Huene, F. von. Los saurisquios y ornitisquios del Cretáceo Argentino. *An*. *Mus*. *La Plata* **3**, 1–196 (1929).

51 Salgado, L., Apesteguía, S. & Heredia, S. E. A new specimen of *Neuquensaurus australis*, a Late Cretaceous saltasaurine titanosaur from north Patagonia. *J. Vertebr*. *Paleontol*. **25**, 623–634 (2005).

52 Voegele, K. K., Ullmann, P. V. & Lacovara, K. J. in *Research Day 2013: Drexel University's 15th Annual Research Day.* 137 (Drexel University, 2013).

53 Gallina, P. A. in *Proceedings of the Third Gondwana Dinosaur Symposium.* (Kellner, A. W. A. & Tomida, Y.) 235–246 (Anais da Academia Brasiliera de Ciências, 2011).

54 Francillon-Vieillot, H., de Buffrénil, V., Castanet, J., Géraudie, J., Meunier, F. J., Sire, J. Y., Zylenberberg, L. & de Ricqlès, A. J. in *Skeletal biomineralization: patterns, processes, and evolutionary trends* (Carter, J. E.) 471–530 (Van Nostrand Reinhold, 1990).

55 Ricqlès, A. J. de, Meunier, F. J., Castanet, J. & Francillon-Vieillot, H. in *Bone 3: bone matrix and bone specific products* (Hall, B. K.) 1–77 (CRC Press Inc., 1991).

56 Chinsamy, A. *The microstructure of dinosaur bone: deciphering biology with fine-scale techniques*. 195 (John Hopkins University Press, 2005).

57 Curry Rogers, K. & Erickson, G. M. in *The sauropods: evolution and paleobiology* (Curry Rogers, K. & Wilson, J. A.) 303–326 (University of California Press, 2005).

58 Huttenlocker, A. K., Woodward, H. N. & Hall, B. K. in *Bone histology of fossil tetrapods* (Padian, K. & Lamm, E.-T.) 13–34 (University of California Press, 2013).

59 Sander, P. M., Klein, N., Stein, K. & Wings, O. in *Biology of the sauropod dinosaurs: understanding the life of giants* (Klein, N., Remes, K., Gee, C. T. & Sander, P. M.) 276–302 (Indiana University Press, 2011).

60 Mannion, P. D. & Otero, A. A reappraisal of the Late Cretaeous Argentinean sauropod dinosaur *Argyrosaurus superbus*, with a description of a new titanosaur genus. *J. Vertebr*. *Paleontol*. **32**, 614–638 (2012).

61 González Riga, B. J. A new titanosaur (Dinosauria, Sauropoda) from the Upper Cretaceous of Mendoza Province, Argentina. *Ameghiniana* **40**, 155–172 (2003).

62 Wilson, J. A. Sauropod dinosaur phylogeny: critique and cladistic analysis. *Zool*. *J. Linn*. *Soc*. **136**, 217–276 (2002).

63 Carballido, J. L., Pol, D., Cerda, I. & Salgado, L. The osteology of *Chubutisaurus insignis* del Corro, 1975 (Dinosauria: Neosauropoda) from the 'middle' Cretaceous of central Patagonia, Argentina. *J. Vertebr*. *Paleontol*. **31**, 93–110 (2011).